Fermi National Accelerator Laboratory

FERMILAB-Pub-91/293-A
October 1991

THE SIGNAL FROM A GALACTIC SUPERNOVA: MEASURING THE TAU NEUTRINO MASS *

Lawrence M. Krauss
Center for Theoretical Physics and Dept. of Astronomy
Sloane Laboratory
Yale University
New Haven, CT 06511

Paul Romanelli
Bankers Trust Co.
1 Bankers Trust Plaza
New York, NY 10006

David N. Schramm
The University of Chicago
Department of Astronomy & Astrophysics
Chicago, Illinois 60637 USA
and
NASA/Fermilab Astrophysics Center
Fermi National Accelerator Laboratory
Batavia, Illinois 60510, USA

Abstract

We have developed a comprehensive Monte Carolo analysis in order to simulate the neutrino signal from a galactic supernova in a large water Cerenkov detector. This allows us to demonstrate that by exploiting the various features of the signal in a way which is largely *independent of the supernova model*, assuming only that the late time behaviour of the signal is flavor independent, a sensitivity to a tau neutrino mass down to the cosmologically interesting range of $\approx$ 25 eV for a medium luminosity burst is possible. This is the case even though the tau signal involves $\approx$ 50 out of $\approx$10,000 total events in a detector of the size of that proposed for "Super Kamiokande". In addition, our results allow us to elucidate several aspects of a supernova neutrino signal in water detectors which had not been previously explored, including new results on the observability of the neutronization burst.

* In press, *Nucl. Phys. B*

Neutrino astronomy completed its neo-natal stage with the observation, on February 23, 1987, of neutrinos from SN 1987a, in the Large Magellanic Cloud [1]. The observation of 11 neutrino events in the Kamiokande II (KII) detector and 8 events in the IMB detector in conjunction with the optical signal from SN 1987a provided the first direct evidence of the central role of neutrino emission in stellar core collapses. Of course, 19 events is not sufficient to allow detailed checking of collapse models, although it is pleasing that many features of the standard theory--in particular, the basic energetics arguments--were at least consistent with the observed signal.[2,3,4]. In order to examine supernova physics in detail, both larger detectors, and closer supernovae will probably be required. Among the new generation of large underground water detectors being planned is the so-called "super-Kamiokande" detector, which will be 10 times larger than KII and have better detection sensitivity and electronics. For a galactic supernova, $\approx$7000 $\overline{\nu}_e$ events might be expected. Also under construction is the SNO heavy water detector in Sudbury, which, while it will be smaller than KII, may achieve sensitivity to neutral current scattering on neutrons, allowing many more non-electron neutrino events to be detected than in light water detectors of the same size. In this work, we shall concentrate on modelling the signal in light water detectors, although we shall make some preliminary remarks about sensitivities in the latter type as well.

Amidst these developments, there has been renewed interest in the possibility that the tau-neutrino may have a cosmologically interesting mass. A neutrino mass in the range of 10-100 eV is large enough so that the cosmic neutrino background could contribute a significant fraction of the mass needed to result in a flat universe today. Also, recent confirmation by Kamiokande of the solar neutrino problem has fueled speculation that the solution may be related to the existence of a muon neutrino mass in the range of 10^{-3} eV [5,6]. If this is the case, a see-saw mechanism for generating neutrino masses from Grand Unified Theories [7] suggests a ν_τ mass as large as O(10) eV, depending on the possible relation of the neutrino mass matrix to the quark and lepton mass matrices.

In spite of the obvious interest in exploring such a mass range, terrestrial experiments are quite limited. The only proposed experiment which might probe such a range is a long baseline neutrino oscillation experiment at an upgraded Fermilab. This, of course, will

depend upon the existence of vacuum mixing between neutrino species. The only possibility for a direct kinematic measurement of a tau neutrino mass in the foreseeable future comes from the observation of tau-neutrinos from stellar collapse. In this case, the travel time from a supernova at ≈10 kpc is such that neutrino masses greater than ≈10 eV will result in dispersive time delays on the order of seconds. Unfortunately, however, tau-neutrinos do not make up the dominant supernova neutrino signal. In a water detector of the size of Super-Kamiokande, for example, we will show that the ν_τ signal will probably involve ≤50 events, out of $\approx 10^4$ total events. Preliminary arguments suggest therefore that distinguishing a cosmologically significant tau neutrino mass will be difficult at best [8,9].

Nevertheless, because of the importance and uniqueness of such a possible measurement, it is worthwhile examining in advance of a galactic supernova what experimenters might do to optimize their sensitivity. In order to examine in detail this issue, as well as the more general question of what might be learned from the neutrino signal from a galactic supernova, we have developed and tested over the past year and a half a comprehensive Monte Carlo program to simulate a supernova neutrino signal, including backgrounds, in underground water detectors. While most of our results will be quoted for a detector with the specifications of Super-Kamiokande, the program is general enough to model any detector. We propose here using several new ideas for isolating and analyzing the tau (and muon) neutrino signals in a way which is independent of the details of supernova models, and relies only on relatively ubiquitous assumptions about the late-time thermal signal. Using our Monte Carlo, we have been able to investigate where these ideas are viable, and if so, what kind of mass limits might be achieved. We report here upon our results. A more detailed description of the program will be published elsewhere[c].

1) The Neutrino Signal:

Neutrino events which are detected in a water detector consist of a measured time, energy and angle for each observed positron or electron. In order to reproduce this signal our Monte Carlo program consists of three stages: in the first a neutrino flux is generated at

[c]A user's manual for the Monte-Carlo and analysis programs is currently being prepared and will appear as a preprint. This, and copies of the program will be available upon request from LMK.

the supernova and propagated to the detector; in the second this flux is convolved with interaction cross sections to determine the scattered events in the detector, involving physical energies and directions; in the third stage the scattered events are combined with information about the detector (and neutrino masses), including the background event rate and spectrum, to generate detected events which are given in terms of their detected time, energy and direction. Each of the latter two stages is generated from the preceding stage by use of a probability distribution. We briefly describe the physics input in each stage:

(a) Neutrino fluxes from Supernovae: The main features of the neutrino flux predicted to arise from stellar collapse have been widely reviewed [10,11]. We describe here those features which we have incorporated into our generation algorithm. The total luminosity in neutrinos in the entire burst is set to vary between 1.5-4 x 10^{53} ergs, which we divide into thermal and non-thermal components. The non-thermal component describes the "neutronization" burst, the initial electron neutrino pulse from the capture of electrons by protons as the shock first hits the neutrinosphere. The time dependence and spectrum of this initial pulse are model dependent, but it generally involves a width $\leq 10^{-2}$ sec. and peak height $\approx 5 \times 10^{53}$ ergs/sec. In the analysis quoted here, the spectrum reported in [10] was fit by a ninth order polynomial, and the luminosity was fit to a gaussian.

After the initial burst, the supernova may enter a phase where matter is accreting onto the surface of the core, and neutrinos are emitted with a thermal distribution. This results in a roughly constant luminosity which we allowed to last between 0.1 and 1 second, with a turn-on width (which we chose as sigmoidal) of $\approx 1/20$ sec. While there is much debate in the supernova community over the explosion mechanism itself [i.e. see 12,13], and the role of accretion, by varying the accretion time between ≈ 0 and ≈ 1 sec, we can accommodate the different possibilities. After this period, no more material is added and so the luminosity falls as the core cools with an exponential decay with a decay constant τ of O(1) second. Each neutrino species has a roughly equal share of the luminosity, although the temperature of their thermal distributions vary. The relative temperature of each species is determined by its interaction length in the supernova core, so that ν_μ and ν_τ have higher temperatures than ν_e. The characteristic temperature scale of the latter is 3-4 MeV and of the former is 7-8 MeV. During the period that the luminosity is constant, the temperature is

set to be constant for all species except for $\overline{\nu}_e$, which increases as neutronization becomes complete. After this there are no longer protons for the $\overline{\nu}_e$ to interact with, so that their interaction length, and hence their temperature, becomes equal to that of ν_μ and ν_τ. We modelled the increase in the $\overline{\nu}_e$ temperature from its initial value T_0 by a sigmoidal function with width of 0.33 sec. We assume that the ν_μ and ν_τ initial temperatures $=2T_0$, and the ν_e initial temperature $=0.9\ T_0$. After the accretion phase the temperatures of all species are assumed to decay exponentially, with a rate proportional to the fourth root of the luminosity decay rate, so that $\tau_T=4\tau_L$. The luminosity and temperature functions of the various species are shown in figure 1 for one sample model.

The neutrino luminosity at the supernova is converted to a flux at the detector using the distance from the earth to the supernova. This distance is variable in the program but we take it to be 10 kiloparsecs in the results quoted here. The end product of the first programming stage is thus a set of four fluxes, which give the number /second· MeV·cm^2 for each of ν_e, $\overline{\nu}_e$, ν_x, $\overline{\nu}_x$, where x here stands for either μ or τ - (Since ν_μ and ν_τ interact identically (to lowest order) in the supernova, their fluxes are essentially identical.) These fluxes are determined by 4 parameters: the length of the accretion phase, t_{mid}, which we varied between 0.1-1 sec; the decay constant for the cooling phase τ, which we varied between 0.5-1.5 sec; the total energy emitted in neutrinos E_0, which we varied between 1.5-4 x 10^{53} ergs; and the intial $\overline{\nu}_e$ temperature T_0, which we varied between 3-4 MeV. In all, we considered 36 different combinations of these parameters, shown in table 1.

(b)Scattering in the detector: The neutrino interactions in water which we incorporated in order to determine scattering events are: a) neutrino scattering off of electrons: ν_e-e^-, $\overline{\nu}_e$-e^- and ν_x-e^-, $\overline{\nu}_x$-e^- (where x again stands for μ or τ); b) electron anti-neutrino scattering off of protons: $\overline{\nu}_e + p \rightarrow e^+ + n$; and c) electron anti-neutrino scattering off of oxygen: $\overline{\nu}_e + {}^{16}O \rightarrow e^+ + {}^{16}N$. For all of the interactions considered, the total and differential cross sections, $\sigma(E_\nu)$ and $d\sigma/dy$, were stored as arrays at discrete values of neutrino energy E_ν. For $\overline{\nu}_e$-p scattering, y is defined to be $\cos\theta_e$, where θ_e is the scattered positron's direction. For all other interactions, y is defined to be $(E_e-m_e)/E_\nu$, where E_e is the scattered electron's energy and m_e is the electron rest mass. Because measurements of both the angle and

energy of the outgoing positrons or electrons will be of vital importance in what follows, we utilized forms for differential cross sections which are more detailed than normally quoted. The general form of $d\sigma/dy$ ($y = (E_e - m_e)/E_\nu$) for (anti)neutrino-electron scattering is,

$$\frac{d\sigma}{dy} = \frac{G_F^2 m_e E_\nu}{2\pi}\left[A_o + B_o(1-y)^2 + C_o\frac{m_e}{E_\nu}y\right]$$

where the parameters A_o, B_o, and C_o are given in Table 2, and G_F is Fermi's constant. The limits $0 < y < 1$, are correct only for ultra-relativistic electrons. For this analysis, however, we incorporated more exact limits, $0 < y < \left(1 + \frac{m_e}{2E_e}\right)^{-1}$. The scattering angle can then be calculated directly from 4-momentum conservation, yielding

$$\cos\theta = \sqrt{\frac{y}{y + 2\delta_e}}\left(1 + \delta_e\right) \qquad (1)$$

where $\delta_e = m_e/E_\nu$ is always a small number for detectable supernova neutrino interactions, since E_ν is generally greater than 10 MeV.

For the reaction, $\bar{\nu}_e + p \rightarrow e^+ + n$, the simplest assumption is that the neutron experiences no recoil. In this limit, the cross section is $\sigma = \sigma_o = \frac{G_F^2}{\pi}(C_V^2 + 3C_A^2)p_e E_e$, where p_e and E_e are the electron momentum and energy, and $C_V = 1.0$, $C_A = 1.25$. The electron energy is calculated simply from conservation of energy: $E_e = E_\nu - \Delta$, where Δ is the proton-neutron mass difference, $\Delta = m_n - m_p$. The electron in this approximation is scattered isotropically. However, as our analysis depends sensitively on angular considerations, we chose to include recoil effects. Following [14], we write $\sigma = \sigma_o(1+\delta_{recoil})$ where

$$\delta_{recoil} = \frac{1}{C_V^2 + 3C_A^2}\left[(C_A^2 - C_V^2)\delta + (C_A - C_V)\frac{\tilde{E}_e(\tilde{E}_e + \delta) + \tilde{p}_e}{\tilde{E}_e}\right]$$

where $\delta = \Delta/m_p$, and we use the notation $\tilde{A} = \frac{A}{m_p}$.

We parametrize the differential cross section by the scattering angle, $\cos\theta$, which varies between -1 and 1 with a nearly flat distribution, and determine the recoil energy from kinematics. E_e, E_ν, and $\cos\theta$ are related by

$$E_e = \frac{E_\nu m_p - \Delta m_p - y^2}{m_p + E_\nu(1-\cos\theta)} \text{ where } y^2 = (\Delta^2 - m_e^2)/2.$$

Again following [14] we find

$$\frac{d\sigma}{d\cos\theta} = g(E_\nu)\tilde{E}_e\left[\frac{1-\tilde{E}_\nu(1-\cos\theta)}{1+\tilde{E}_\nu(1+\cos\theta)}\right]f(\tilde{E}_\nu, \tilde{E}_e)$$

where

$$f(\tilde{E}_\nu,\tilde{E}_e) = (C_V+C_A)^2\left(\tilde{E}_e + \delta + \frac{\delta^2}{2}\right)\tilde{E}_e + (C_V-C_A)^2\left(\tilde{E}_\nu - \delta - \frac{\delta^2}{2}\right)\tilde{E}_\nu - (C_V^2-C_A^2)(1+\delta)\left(\tilde{E}_\nu - \tilde{E}_e - \delta - \frac{\delta^2}{2}\right)$$

and $g(E_\nu)$ is fixed by the normalization of $\sigma(E_\nu)$.

Finally, for completeness, we included the interaction of $\bar{\nu}_e$ with oxygen, $\bar{\nu}_e + {}^{16}O \rightarrow e^+ + {}^{16}N$. We assumed that the cross section is only non-zero above some threshold energy, E_{thresh}, and has the form [11]:

$$\sigma(E_\nu) = 5\cdot10^{-43}\text{cm}^2\left(\frac{E-E_{thresh}}{10\text{ MeV}}\right)^2$$

where, for this reaction, E_{thresh} = 13 MeV. The energy of the scattered positron is given simply by the energy difference $E_e = E_\nu - E_{thresh} + m_e$. The recoil of the oxygen atom is negligible, so the positron is released roughly isotropically.

We used these differential cross sections to calculate scattered events as follows: Our program has discrete time steps: 150 steps for $0 < t < 0.1$ seconds and 900 steps between $0.1 < t < 50$ seconds. (The smaller step size in the early time region is to study the initial electron neutrino burst.) For each time value, the neutrino energy is stepped through from 0 to 100 MeV in 300 steps (the highest precision possible due to memory constraints). At every energy and time value, each neutrino type is considered in turn, and for each neutrino all relevant interactions are calculated sequentially. For generating events we then started with time, neutrino energy, neutrino type and interaction type. The specific neutrino fluxes discussed above were used to generate a spectral flux of neutrinos (#/MeV/sec/cm^2) for each specific time and energy. These values were used to generate r, the expected number of events for this time and energy bin, neutrino type and interaction type, where r = flux · cross section · # scattering centers · dt · dE. The number of scattering centers depends on the interaction involved, and was set equal to $f \cdot 10^{33}$, where $1.07\cdot10^{33}$ is the number of molecules in 32000 metric tons of water (the fiducial volume of the Super-Kamiokande detector) and f is the number of scattering centers per water molecule: f = 10 for scattering off electrons; f = 2 for scattering off protons; and f = 1 for scattering off oxygen.

The expected number of events, r, was used to randomly generate an actual number of scatterings, n, for each bin, using Poisson statistics. Having determined the number of

events, n, in each bin, which are the result of a specific neutrino type and interaction, we then used the differential scattering cross sections to randomly generate an energy and direction for each scattered electron or positron, as follows: For a fixed incident neutrino energy, the differential cross section $d\sigma/dy$ is directly proportional to the probability distribution in y, dP/dy. We randomly generated values of y by integrating each differential cross section, equating the integral to an integral over a flat distribution, and then inverting the equation. The distributions were integrated and inverted numerically, and then stored in files to be used each time a new supernova burst was generated. We stored the inverted distributions in the form of equal probability intervals, which allowed rapid calculation of the randomly generated value, y. This process was repeated for each time-energy bin. The end result was a set of scatterings identified by: release time; incident neutrino energy; scattered electron (positron) energy and direction; and neutrino type.

(c) Detected Events: Determining detected values involves two different issues. First, the detector has certain energy and angular resolutions, as well as a trigger level and a threshold, and also a background event rate. Thus, not all scatterings are detected, some detections are background related, and the detected energy and direction are not identically equal to the incident physical values. Second, the timing of detections is altered if the neutrinos have masses.

Our detector is patterned after the proposed Super-Kamiokande detector, a very large water Cerenkov detector 41 meters high and 38 meters wide, with a total mass of 50,000 metric tons and a fiducial volume of 32000 tons of water. (A more complete description of Super-Kamiokande can be found in Ref. [15].) The detector is sensitive to neutrinos from many possible sources. We consider Cerenkov light both from positrons ($\bar{\nu}_e+p\rightarrow e^++n$) and recoil electrons ($\nu+e\rightarrow\nu+e$). The detector has an energy threshold, E_{th}, below which no electrons are detected. Above this value the trigger gives the probability of detection as a function of energy. The sigmoidal trigger function we used varied smoothly from $P(E_{th})=0$ to $P=P_{max}$, with a width given by E_b. We determined these parameters by fitting to the trigger given in Ref. [16]. The parameter values which fit this form best are: $P_{max} = 1.0$; $E_{th} = 4.5$; $E_b = 0.5$. We used this trigger function as a probability distribution to randomly determine whether a scattering above threshold was detected

Once a scattering is detected it is necessary to generate values for the energy and direction recorded by the detector. The detected energy values were generated randomly assuming a gaussian probability distribution with width σ_E about the physical energy E_e, where σ_E is a function of E_e taken from [16] to be: $\frac{\sigma_E}{E_e} = \frac{13.8\%}{\sqrt{E_e/10\,\mathrm{MeV}}}$.

The situation is a little more complex for generating the detected direction of scattering, given in terms of the initial supernova direction. We assume a gaussian angular resolution function, $\frac{dP}{d\Omega} = \frac{1}{\sqrt{2\pi}\sigma_\theta} \exp\left[\frac{-\alpha^2}{2\sigma_\theta^2}\right]$, for the probability of detection within a solid angle $d\Omega$ of the physical scattered direction, with width σ_θ. Here $d\Omega = \sin(\alpha)d\alpha d\varphi$, where α and φ are angular coordinates *with respect to the scattered direction*, and σ_θ is a function of E_e (by assumption σ_θ is small enough so that the probability of detecting $\theta > \pi$ is negligible). One can easily use this resolution function to generate α (the azimuthal angle φ is not relevant). The challenge is to express the detected direction not in terms of unmeasured angle α, but in terms of the measured angle, θ_d, from the supernova. A tedious but straightforward calculation, gives: $\cos(\theta_d) = \cos(\theta_e)\cos(\alpha) - \sin(\theta_e)\sin(\alpha)\cos(\varphi)$, where α and φ are as above, and θ_e is the physical scattered angle from the supernova. One thus first randomly generates α, and uses this expression to determine θ_d.

The absolute angular uncertainty, σ_θ, is governed in part by finite detector resolution, but is mostly due to multiple electron scatterings in water. Consequently, the angular resolution cannot be much improved from the KII detector. Experimenters parametrize the angular uncertainty by a root mean squared angle. If σ_θ is small enough, it can be related to the root mean squared angle: $\langle\theta^2\rangle^{1/2} = \sqrt{2}\sigma_\theta$. The dependence of $\langle\theta^2\rangle^{1/2}$ with energy for the KII detector is given in [16], and we fit this to a ninth order polynomial, shown in figure 2.

Next, the detector has background events which are unrelated to the supernova. The spectrum and rate are given by on line studies of the detector, and clearly there is not yet information on the background rate in future detectors. As an estimate of the possible background, we took the background for the KII detector, fitted its energy spectrum and scaled up the rate by a factor of 25%, with the result shown in figure 3. While we expect the Super-Kamiokande background to be larger than the KII background (simply because the mass is larger) the improved electronics and improved photosensitive coverage will also

cut it down. In any case, we used this spectrum to randomly generate background event times and energies, which were also assumed to be isotropic. Our results are sensitive to the background and a more precise value is needed to make absolute statements. However, the results presented here will not be altered substantially unless the actual background is more than about ten times bigger than what we have assumed.

Finally, the time stored with the detection is the time that the neutrino is released from the supernova. There is a constant time-of-flight delay factor for all neutrinos, which is neglected. Since one goal of this analysis is to determine what kind of neutrino mass limits might be obtained from water detectors, we allow an *additional* time-of-flight delay if neutrinos have a mass which goes like $\Delta t_2 = \frac{1}{2}\frac{D}{c}\frac{m_\nu^2}{E_\nu^2}$, assuming $m_\nu \ll E_\nu$. This delay is added for each massive neutrino event. The advantage of this procedure is that we can generate a set of events from a supernova explosion, and then afterwards operate on this set to explore the effect of any mass we wish, without having to re-run our Monte Carlo.

Thus we obtain, for each supernova explosion, a set of detected events, with each consisting of a time, energy and direction. These come from all the interactions of all species of neutrinos, and also include background events. Sample signals for several different explosions, showing the time signal, and energy spectrum are given in figure 4.

2) Analysis Strategy:

Using our Monte Carlo we can examine in great detail many features of the neutrino signal predicted to arise from a galactic supernova. Here, however, we are most concerned with features which can probe the time delays due to a non-zero tau neutrino mass. We considered, for reasons soon to be discussed, a range of ν_τ masses, from $m_\nu = 0$ to $m_\nu =$ 1KeV. To get some idea of the possible signatures, we present, in figure 5, delays for representative masses within this range as a function of energy. Since the characteristic energy for ν_τ is 18-24 MeV, if the mass of ν_τ is greater than around 500 eV these neutrinos will be delayed beyond the limit of our consideration. The only way to probe masses beyond this is if the absence of these τ neutrino events can be measured. For masses between 50 eV and 400 eV, the effect of the mass will be to push events from the first

second or so of the signal to 5-50 seconds. The challenge is to see if this effect can be statistically distinguished, if only a few such events are observed.

On first thought, such a possibility may seem remote, especially for masses in the 10-50 eV range. The largest signal in the detector by far will be from $\bar{\nu}_e + p \rightarrow n + e^+$, although all neutrino species will contribute from $\nu + e \rightarrow \nu + e$. Approximately 5000-15000 $\bar{\nu}_e$ events are expected, versus 30-100 ν_τ events. Moreover, part of the purpose of the supernova observation will be to pin down the parameters of the supernova explosion. Without pre-ordained knowledge of these parameters, how can we hope to distinguish neutrino mass effects when fitting model predictions to the explosion? To graphically demonstrate this difficulty, we show in figure 6 a histogram for all detected events for one model explosion, with the ν_τ mass set to 0 in one case and to 400 eV in the other. The two results appear identical!

Nevertheless, we believe one can surmount these difficulties, and extract the ν_τ signal by exploiting two kinematic characteristics of the neutrino signals, one of which goes against previous intuition:

(1) First, an angular cut on the data removes most of the $\bar{\nu}_e$ signal. As demonstrated in equation (1), neutrino-electron scattering at MeV energies is peaked strongly in the forward direction. For example if a scattered electron is produced with only 10 MeV from a neutrino with incident energy E= 20 MeV the scattering angle will be $\cos\theta \approx 0.95$. By contrast, the positrons produced by $\bar{\nu}_e$'s are nearly isotropic, with in fact some mild peaking in the rearward direction. Thus, we should search in the forward cone for the tau neutrino signal. In principle, while one can gain in "signal to noise" by reducing the size of this forward cone (until one runs out of events), in practice the smallest reasonable choice in opening angle corresponds to the angular resolution of the detector itself. For incident ν_τ's with mean energy ≈25 MeV, the mean scattered electron energy is ≈12 MeV. The angular resolution σ for electrons of this energy is [16] $\approx 18^0$. Thus, we define the forward cone as corresponding to $\cos\theta > \cos(18^0) \approx 0.95$. To get an idea of how much more clearly the signal for a tau neutrino mass appears in this forward cone, we display, in figure 7, histograms of events in this cone for one model explosion, as the ν_τ mass is increased from 0 to 400 eV. The migration of events to later times is clearly visible.

(2) Convention wisdom suggests that the ν_τ and ν_μ events will have higher mean energy than $\bar{\nu}_e$ events because the former are emitted from the supernova with higher mean temperature. However, *exactly the opposite is true*. Because the y-distribution in neutrino electron scattering is flat, the average energy of the scattered electrons will be half that of the incident neutrinos, whereas in $\bar{\nu}_e$ - p scattering the outgoing positron takes up almost all the energy of the neutrino. In addition the $\bar{\nu}_e$ - p cross section goes as E^2, while the ν - e cross section goes as E. This serves to further enhance the high energy tail of the positron spectrum. As a result of these two factors, the $\bar{\nu}_e$ signal occurs at systematically higher energies, and we can hope to further suppress the $\bar{\nu}_e$ background by making an energy cut. Indeed, without this cut, we shall see that it is impossible to demonstrate statistically the existence or absence of the entire ν_τ signal.

While the ability to isolate the overwhelming $\bar{\nu}_e$ signal is very important for extracting the tau neutrino signal, it more importantly provides the essential ingredient which allows a supernova model-independent limit on the tau neutrino mass. By breaking up the signal in to "forward" and "rearward" signals (i.e. $\cos\theta<>0.95$), *we can analyze the internal consistency of the signal itself.* In particular, we may use the 5000-15000 events in the rearward cone to provide a fit to the parameters of any sufficiently complex model at the 1% level. We may then compare this fit with a fit to the data in the forward cone. For several key parameters, in particular those governing the late time behavior, *which we assume is flavor independent* (based on thermal emission), the fits should be identical in the absence of a neutrino mass. The extent to which they disagree then allows us to probe for such a mass. We cannot stress too strongly that the beauty of this procedure is that it is largely independent of what the actual supernova model is. As long as the model which fits the rearward data is sufficiently complex (incorporating the basic supernova physics) to provide a sufficiently good fit to the rearward data, it should provide a good fit to at least the late time behavior of the forward data in the absence of neutrino masses. One must, of course, take into account that the smaller forward data set limits the statistical accuracy of any fit. Nevertheless, since all late time events will essentially fall in this forward cone, containing far fewer events than the total, even 5-6 such events can be statistically quite significant. In any actual experiment, we expect that experimenters would fit several

different models to the rearward data in order to extract the best fit. What we show here is that even a single simple fitting algorithm allows one to determine statistically a non-zero tau neutrino mass. We can also demonstrate which techniques are likely, or not likely to be fruitful in this regard. The only assumption in this whole procedure is that the late time supernova signal is independent of neutrino type. Since this late time behavior is based on thermal cooling, such an assumption seems to be one of the safest one can make.

3) Analysis and Results:

Using the strategy outlined above, we fit the detector events generated by our Monte Carlo program for the 36 supernova models to a simple 5 parameter model using a maximum likelihood technique. The supernova model we used to fit the data was simpler than the model used to generate the events. The luminosity function consisted of a constant term L_0, for a time t_{mid}, followed by an exponential decay with time constant τ. The main difference between this and the model which generates the data is the lack of a "turn-on" term. Each species is assumed to share the total luminosity E_0. The temperature functions we assume for the model are the same as for the generating model, with a single parameter T_0, except for $\bar{\nu}_e$, which is assume to have a simple linear increase, achieving the same temperature as the muon and tau neutrinos after time, t_2 (compared to the sigmoidal increase in the generating model).

The luminosity and temperature functions were used to generated a spectral flux function for each neutrino: $d^2F/dEdt$, which was then convolved with a differential cross section to yield the rate for producing scattered electrons (positrons) of energy E_e, i.e. d^2N/dE_edt. This was then multiplied by the probability for detecting an electron (positron) with energy E_e, obtained by multiplying the threshold and sensitivity functions. Finally, we integrated this function over a gaussian resolution function for the energy E_e, to obtain the detection rate function d^2N/dE_ddt. This is the expected detection rate for a single neutrino type and interaction. We repeated this process for all neutrinos and their interactions, and added the results, along with a similar expression for the observed background rate, to get the total expected detection rate.

While in principle this procedure is straightforward, in practice the determination of

$d^2N/dE_d dt$ in each bin involves a triple integral which cannot be evaluated analytically, and would be prohibitive to perform numerically. Instead, the integrals were evaluated at discrete values of E_d, for representative values of the temperature for unit luminosity. The actual values of $d^2N/dE_d dt$ were then found by interpolation between temperature values, and scaling by the appropriate luminosity.

In order to incorporate the angular information which is essential for extracting the tau neutrino signal, we divided the data into a forward cone, and a rearward cone, as defined earlier, and computed a separate likelihood function based on $d^2N/dE_d dt$ for each cone. Since the detected angle is itself a function of the actual scattered angle, fixing the event rate in the forward cone is somewhat subtle, but can be achieved using the relation given earlier between actual and detected scattering angles.

The likelihood function in each region is given by

$$L = \sum_{i=1}^{N_{data}} \ln\left(\frac{d^2N}{dE_d\, dt}\right) - N_{model}$$

where the index i runs over all bins containing an event, and N_{model} is the expected total number of events from the fitting model. The bin size is set so that there is at most one detected event in any bin. The best fit parameter set is then determined by maximizing L.

We remind the reader that the point of this analysis is to look for a signal in the forward direction that is identifiably different from what is implied based upon an analysis of the rearward data. Before performing detailed statistical tests, we begin by merely examining the fits to the rearward and the forward data for a sample explosion. Shown if figure 8(a) is the prediction of the best fit to the rearward data superimposed upon the actual data for a model explosion, with zero tau neutrino mass. As can be seen, the fit is good, except perhaps for early time differences, due to the simple linear increase in the fitting model compared to the sigmoidal increase in the generating model. Even so, the fit is quite good. FIgure 8(b) shows the fit to the forward cone for the same explosion, and also the prediction based on the fit to the rearward cone. As can be seen, both predictions are in good agreement, and the both agree with the data. In Fig 8(c) and (d) the same procedure is applied, but now the tau neutrino is given a mass of 100 eV. The histogram in 8(c) appears on this scale to be virtually identical to the histogram for zero neutrino mass in

8(a). However, in 8(d), in which the forward data is displayed, it can be seen that the rearward fit matches neither the forward data, nor the fit to the forward data. The rearward events cannot account for the anomalous late-time events in the forward cone, which are now clearly observable. It merely remains to quantify this, in order to determine what kind of neutrino masses can be distinguished. We now discuss three techniques we have so far employed to investigate this issue.

(a) Likelihood matching: This technique is a simple extension of the comparison of forward and rearward fits describe above, which allows a quantitative analytic comparison of fits. One way to go about such a procedure would be to define confidence limits about the two best fit points in parameter space, and then compare the overlap. The ideal way to do this would be to determine the 5-parameter surfaces of constant likelihood for the two fits, and then compare them directly for overlap, and integrate the product of likelihoods over parameter space to get a conditional probability. Unfortunately, to determine 5-dimensional contours with any precision would require at least $\approx 20^5$ points to be evaluated in likelihood space. This would take years of continuous processing on a Vax11-780 to analyze a single run of a single model.

Nevertheless, we can do almost as well by a much simpler procedure, as a result of the structure of the two likelihood functions. Because the rearward fit is based on 50-100 times more events than the forward fit, it is much more sensitive to changes in parameters. As a result, the overlap of confidence intervals should resemble fig 9(b) more than 9(a). Thus, a good approximation to the conditional probability can be obtained by finding the likelihood of the best rearward fit, assuming the forward fit. Specifically, we use the best fit parameters calculated for the rearward fit in the likelihood function for the forward data, and subtract from this value the value obtained using the best fit parameters for the forward fit in the same likelihood function. This gives, by straightforward statistical rules, the likelihood of the rearward fit, assuming the forward fit is correct. We then repeated this procedure for a number of different neutrino masses. In figure 10, we show our results, for 3 different supernova bursts-one with high luminosity, another with low, and a third with different time structure, using the definition of the forward cone and rearward cones given earlier, and including all the forward events, with no energy cut. These results are

mixed. For masses ≈40-400 eV[d] we can find strong disagreement between the forward and backward results for some mass values, but instead of the monotonic rise, and then fall we would expect, there are valleys where the disagreement is much smaller. This is due to two effects. First of all, if there are late time tau neutrino events which occur in the rearward cone, the rearward fit can be shifted in the direction of the forward fit. Second, if there are enough late-time events in the forward direction, all fits will be bad. This will flatten the likelihood region, allowing a broader range of "acceptable" values. We can reduce the first effect, by reducing the size of the "rearward" cone, so that it is not contaminated by forward tau neutrino events. The removal of the forward tau neutrino "contamination" more than outweighs the effect of reducing the statistics in the rearward cone. In figure 11, we show the plots obtained by reducing the rearward cone to $\cos\theta<.80$ for two model explosions. The sharp valleys disappear.

The second effect, that of all zero mass models providing a poor fit to the forward direction can be reduced by using not a best fit but a goodness of fit technique. By binning the events differently, so that there are many events per bin, a chi-squared analysis could be used to examine whether any non-zero mass model provides an acceptable fit. Better still, we can add a mass parameter to the fitting function, and either perform a best fit for this parameter, or compare the improvement of fits with this extra parameter using an F-test, which quantifies the affect of adding another variable. All of these improvements are currently under investigation. Nevertheless, as figure 10 demonstrates, depending upon the supernova luminosity (and distance), this technique can already yield a sensitivity for masses in the range ≈40-400 eV.

(b) Late time events: Our second technique is to look directly for late time events. The best fit to the rearward data is used to generate a predicted number of events in the forward direction. We then use Poisson statistics to compare the expected number with the actual number after some time t_{cut} and before 50 seconds. This approach is very model-independent, because it depends only upon the large statistics model fit to the late time behavior of the rearward signal. Also, while it is not independent of the other test, it is

[d] For masses larger than O(100) eV, standard cosmological arguments suggest a heavy neutrino should be unstable. The sensitivity to larger masses quoted here is based on the assumption that the decay time is long compared to the travel time. We shall discuss the alternative possibility later in this article

somewhat complementary---in that the presence of many late time events in the forward direction improves the sensitivity of this test, when it can reduce that in the former.

We display the results for several representative models in figure 12. In each case we reprocessed the same data set for each model while increasing the tau neutrino mass, and used four values of t_{cut}, 4.5, 9.5,14.5, and 19.5 seconds. The expected number shown is the integrated rate between 4.5-50 seconds for zero mass for the best fit parameters (thus, for later times, this over-estimates the event rate). The values P(n) are the Poisson probabilities for find n *or more* events, given the expected background number.

Our results are encouraging, although they are more luminosity dependent. As can be seen, for a medium luminosity burst (model 17) (at 10 kpc) with short accretion time (0.1 sec), a non-zero mass is indicated at the 99% confidence level for masses between 50-350 eV, and even for masses down to ≈25 eV and up to ≈425 eV, the signal is noticeable at the 90% confidence. If the luminosity of the burst is reduced to the lowest expected, however (model 4), sensitivity at the 99% confidence level is restricted to the range 75-150 eV. Similarly, if the constant luminosity phase is longer (1.0 sec--model 23), the accessible range is somewhat reduced, to ≈60-325 eV.

We note that these results, demonstrating a possible sensitivity to a mass range ≈30-400 eV, have been obtained *without any energy cuts, and without any correlation of energy of events with time, nor do they take into account the spectral differences between the background events and supernova events.* Also, as we indicated earlier, this analysis is not independent of the maximum likelihood fitting analysis performed earlier. When these statistical analyses are combined, we expect the robustness and range of the lower and upper limits will increase. In particular, we expect that putting a mass parameter in the maximum likelihood fits should improve sensitivity to the energy dependence of the late time events. We also need not restrict the interval to 4.5-50 seconds, which is the period dominated by the background events. As we include more modelling of the rearward signal in the late time analysis we can make the lower cutoff earlier, thus improving sensitivity to still smaller masses. Hence, given the sensitivity down to a mass ≈30-50 eV of our preliminary tests, a statistically significant sensitivity down to masses at as small as ≈25 eV should be possible, depending upon the supernova luminosity and timing, as measured in

the rearward signal. We made preliminary steps to examine this, by incorporating the same energy and rearward cuts here as were used earlier, and lowering the cutoff time. We can see in figure 13 a sensitivity to masses as low as 25 eV. Incorporating a time interval past 50 seconds could in principle increase the upper end of the sensitive range, although beyond ≈400-500 eV the events are so spread out as to approach the background event rate. It is possible however that using the spectral difference between supernova and background events might allow some distinction between signal and noise to be made. Finally, note that because the time delay is proportional to mass *squared*, even if the actual cooling decay constant were twice as large as the largest investigated here, the lower bounds on mass sensitivity would only be expected to increase by a factor of ≈1.4.

(c) Missing Events: For masses in excess of ≈ 1 keV, what may be most noticeable about the tau neutrino signal is the lack of one! If events are delayed beyond the detectable limit, we should look for a *deficit* of events in the forward direction. Sensitivity to such heavy masses has become more urgent with the rebirth of indications of a 17 keV neutrino state mixed with the electron neutrino [17]. Of course, such a neutrino will produce events which are delayed by more than 50 seconds only if it does not decay to lighter states on its way from the supernova. For lifetimes which are short compared to the travel time, the observed signal could be determined by multiplying each event with zero mass by a time delay determined by the actual distance travelled before neutrino decay. This distance could in turn be determined by a Monte Carlo which utilizes the time dilated lifetime based on the neutrino energy. The effect of such decays would be to move more events into our 50 second window, increasing sensitivity to such a mass. We have not explicitly considered this possibility here, however, since it depends sensitively on neutrino lifetime. Instead, we concentrate here on the more difficult task of searching for a signal delayed beyond the event window we have chosen.

A fact which is not often emphasized about even the purely forward events, is that they are dominated by electron neutrino events, by a factor of almost 10 to 1. This is due to the enhancement of these interactions by the inclusion of charged, as well as neutral current scattering. Thus, to be sensitive to the absence of a tau neutrino signal, we must have statistically accuracy in the range of 10%-implying the need for >O(100) forward scattering

events. Moreover, as we briefly discussed earlier, even the forward scattering signal is, due to the angular resolution of the detector, dominated by $\bar{\nu}_e$ events. Hence, without use of the energy cut proposed earlier, there is no way to probe for the non-existence of the tau neutrino signal in light water detectors (we shall discuss the situation at SNO later). This is graphically demonstrated in figure 14, where we display the integrated spectrum for "forward events" based on the best fit to the data for zero mass for a representative burst. As we can see, however, if we make an energy cut, we can eliminate only a fraction of the tau neutrino events, while eliminating the bulk of the $\bar{\nu}_e$ events. We chose two different cuts, $0<E<15$ MeV, and $0<E<12$ MeV.

We use the best fit parameters to generate an expected number of events in the forward direction (including the energy cuts), and compared it to the actual number. It turns out, because the best fit parameters have a statistical uncertainty on the order of 1%, that the uncertainty in the predicted number is dominated by Poisson Statistics, and is hence $\approx\sqrt{N}$. In table 3 we display the expected number and the actual number of forward events for several models,for m=0 and m=1 keV, and for the two energy cuts.

The general results are clear. If the luminosity is large, i.e $N\geq100$, the deviation between the predicted and "actual" number of events is just barely significant at the 2σ level. This would imply m>O(500) eV, but gives no more detailed information about the actual mass. This result suggests more generally that light water detectors may not be able to distinguish between 2 and 3 neutrino species, unless the supernova is of above average luminosity (or closer than 10 kpc). As a result, unless specific timing information on events delayed greater than 50 sec can be extracted---either by a reduced background event rate, or using spectral information to distinguish signal from background, a sensitivity to a tau neutrino mass in excess of ≈1 keV is not assured using light water detectors.

(d) The Early time Signal: While not directly related to the analysis described above, our work sheds light on an issue which has received some attention in the past. It has been suggested that because the dispersion due to neutrinos of ≥O(eV) is O(sec), that the early time signal--namely that of the supernova "turn-on"--either the early neutronization burst last O(10 msc) or the O(.05) sec turn on for the thermal burst---might allow the strongest sensitivities to small neutrino masses[18,19]. We show here that such early time structure

is not likely to be probed using light water detectors. We display in fig. 13 the early time forward cone events for a represented, average luminosity model. We see that in spite of the potential sensitivity of the neutronization burst to small electron neutrino masses, we find that there *is no signal for the neutronization burst.* This somewhat surprising result, is upon reflection, clear. The total number of expected events from the neutronization burst, even for a detector of the size of Super-Kamiokande, is O(1)!. Thus there is no way this signal could ever stand out, even against the thermal turn-on signal. More generally, the neutronization burst has a luminosity of O(5 x10^{53} ergs/sec), only slightly greater than that in the thermal burst. However, since the ν_e-e cross section is at least 10 times smaller than the $\bar{\nu}_e$-p cross section, even if there were more than 1 event for the neutronization burst, it would be difficult to extract this from the thermal turn on in a light water detector.

Regarding the second issue, we also see from figure 15 that there is no discernible effect of a tau neutrino mass on the early time signal. This is because the ν_τ signal is hopelessly small compared to the $\nu_e + \bar{\nu}_e$ signal, even with angular and energy cuts. Thus again, since there are O(1) events in each 10 msec interval in the early stages of the explosion, any effect of a ν_τ mass is well below "background" in the early signal. As our analysis demonstrates, the place to look for a ν_τ mass in a light water detector is not at early times, but at late times, where delayed events may stand out by their presence or absence.

Conclusions and Extensions:

Our comprehensive Monte Carlo has allowed us to elucidate many new features of the neutrino signal for a galactic supernova in a water detector. In particular we have shown that using the kinematic features of the neutrino interactions allows general a sensitivity to a ν_τ mass in the range of at least ≈50-300 eV, and depending upon the luminosity (distance) of the supernova, masses down to ≈20-25 eV may be probed. The statistical analysis presented thus far is in some sense preliminary. It was designed to probe what general range of masses the detection of a supernova burst might be sensitive to. As we have discussed, more sophisticated tests, including incorporating a neutrino mass in the maximum likelihood fits, utilizing energy cuts in the late time analysis along with exploring earlier parts of the signal in this analysis, are now being performed, and indications are that

they should extend the mass range for which a neutrino mass might be detected.

We have also examined what kind of improvements in the Kamiokande detections strategy might further increase the range of sensitivity. Without question, if the angular resolution could be improved, the results would improve as well. Unfortunately, the angular resolution is largely determined by multiple scattering of electrons, and is thus not likely to be accessible to improved detection technology. Energy resolution is already quite good, and it is unlikely that improvements in this, even if possible, would have much effect. A lower threshold would both increase the number of events for low luminosity bursts, and allow larger delays for a fixed mass. The former effect could improve the statistics for the "missing event" analysis, and the latter might improve both the maximum likelihood and the late time sensitivity to smaller masses. To check the former, we performed the analysis in (c) again, using improved energy resolution (by 20%), and a smaller trigger energy (3.5 MeV). Unfortunately the results did not change significantly in this case. We are currently exploring the latter effect. Perhaps the most direct improvement would be to further increase its size, but this may also be prohibitive.

What about other detectors then? The most exciting new development in this regard involves the construction of the Sudbury Neutrino Observatory (SNO) heavy water Cerenkov detector [20]. While this is much smaller than Kamiokande, it is possible that neutral current fission of deuterium may be observable. In this case, non-electron (anti) neutrinos would have cross sections which are approximately as large as the $\bar{\nu}_e$-p cross section. Thus, they would contribute a much large fraction of the signal, and it has been argued that this might improve sensitivity to the tau neutrino. We are currently incorporating the features of the SNO detector in our Monte Carlo to examine this issue in detail.

We do however have some preliminary thoughts in this regard. As far as the analysis we have thus far performed, its strength lies largely in the existence of the signal from the $\approx$10,000 $\bar{\nu}_e$-p events in the large detector. In SNO, one would expect a total of perhaps 500-1000 events from a galactic supernova. Thus, by itself, it is not clear that the SNO detector could take advantage of the strategy we propose here to provide limits on the ν_τ mass. However, in co-ordination with the fitting analysis which could be performed at a

Super-Kamiokande detector, the possible neutral current signal at SNO appears at first glance to provide a very useful potential extra handle.

Nevertheless, even in this case, it is not clear, without a detailed analysis of the type we have performed here for light water detectors, whether the SNO signal could improve the systematics and statistics. While the neutral current events are clearly distinguishable from charge current events when taken one at a time, the average time for neutron capture in the detector is estimated to be ≈5-10 msec. Thus, if events are being recorded at a rate exceeding ≈100/sec, it is not clear that the neutron capture signal can be unambiguously associated with a specific electron or positron signal. Moreover, the neutral current dissociation signal carries little or no energy information. It may be that these problems are not severe. It is, after all, the late time events which are most significant for our analysis, and here the event rate is small enough so that neutral current events can probably be distinguished---even if the maximum likelihood analysis will be hampered by the loss of energy information. In any case, we are currently investigating these issues in more detail.

To conclude then, our analysis has shown that, contrary to naive expectation perhaps, with some luck, the next galactic supernova may provide a signal in large underground water Cerenkov detectors which could allow detection of a cosmologically significant ν_τ mass. More importantly, perhaps, it has demonstrated that in this issue, it is the details which count! Without a detailed analysis of the actual signatures, important features of the signal can go unnoticed, or at least cannot be exploited.

Acknowledgements: We thank T. Koshiba, K. Lande, A. Mann, G. Beier, and A. Suzuki for helping provide information on the Kamiokande detector, and J. Wilson, and R. Mayle for discussions on supernovae. We also thank R. Lehrer, who has helped in the development of several of the computer routines and testing procedures we utilized.

This work was supported in part by NSF, DOE, Texas National Research Commission and the Foundation for Physical Science at Yale University; by NSF, DOE and NASA grant #NAGW 1321 at the University of Chicago; and by DOE and NASA grant #NAGW 1340 at the NASA/Fermilab Astrophysics Center.

References:

1. K. Hirata et al. , Phys. Rev. Lett., **58**, 1490 (1987); Bionta, R. M., et al. , Phys. Rev. Lett., **58**, 1494 (1987).
2. e.g. see L. M. Krauss, Nature, **329**, 689 (1987)
3. e.g. see D. N. Schramm, Comments Nucl. Part. Phys. **17**, 239 (1987); for further references to SN1987a see D.N. Schramm, J. Truran , Phys. Rep. **189**,89 (1990).
4. for a recent complete quantitative analysis see T.J. Loredo and D. Q. Lamb, Annals of the New York Academy of Sciences, **571**, 601 (1989), and references therein.
5. i.e see J. N. Bahcall and H. Bethe, Phys. Rev. Lett. **65**, 2233 (1990)
6. a recent updated analysis has been performed by E. Gates, L. M. Krauss, M. White, YCTP-P26-91, submitted to Nature.
7. M. Gell-Mann, P. Ramond, R. Slansky, in *Supergravity: Proc. of Supergravity Workshop,* Stony Brook, ed. P. Van nieuwenhuizen and D. Z. Freedman (Amsterdam: North Holland), p. 315 (1979): T. Yanagida, Prog. Theor. Phys. **B315**, 66 (1978)
8. i.e. see D. B. Cline et al, UCLA preprint APH0020-UCLA-1/90 (1990)
9. e.g. see D. Seckel, G. Steigman , T. Walker, Ohio State preprint OSU-TA-1/91 (1991)
10. R. Mayle, J.R. Wilson, D.N. Schramm, Ap. J., 318, 288 (1987).
11. A. Burrows,, Ann. Rev. Nuc. Part. Sci., 40, 181 (1990)
12. H. Bethe, G. Brown, Sci. Am. **252**, 60 (1985)
13. J.R.Wilson, R.Mayle, S.Woosley, T.Weaver, Ann. N.Y. Acad. Sci. **470**, 267 (1986)
14. P. Vogel , Phys. Rev., D29, 1918 (1984).
15. T. Kajita, T. ,University of Tokyo report ICR-Report-185-89-2 (1989); Totsuka, Y. in Seventh Workshop on Grand Unification, ed. by J. Arafune, , World Scientific, (Singapore 1990)
16. M. Nakahata, U. Tokyo Ph. D. Thesis, UT-ICEPP-88-01; also A. Suzuki, private communication
17. i.e see A. Hine and N. A. Jelley, Phys. Lett. 257B, 441 (1991)
18. D.B. Cline et al, UCLA preprint APH0020-UCLA-1/90 (1990)
19. D. Seckel, G. Steigman , T. Walker, Ohio State preprint OSU-TA-1/91 (1991
20. G.T. Ewan et al, *Sudbury Neutrino Observatory Proposal,* SNO-87-12 (1987)

Figure Captions:

Figure 1: An example of the temperature and luminosity functions for the various species, for one model supernova explosion (model 17)

Figure 2: Angular uncertainty parametrized by $\sqrt{\langle\theta^2\rangle}$ ($=\sqrt{2}\,\sigma_\theta$) for the Kamiokande II detector [16], and our fit.

Figure 3: Background rate for Kamiokande II detector [4] scaled by 1.25, and our fit.

Figure 4: Samples of the detected signal for several supernova bursts, showing the time structure and energy spectrum.

Figure 5: The time delay, as a function of neutrino mass and neutrino energy, for a burst at 10 kpc.

Figure 6: Histograms for all detected events for one model, for m_ν=0 and 400 eV.

Figure 7: Histograms for events in the forward cone, for the same model, as the neutrino mass is increased from 0 to 400 eV

Figure 8: The best fit predictions superimposed on the "actual" neutrino signal for one model. (a) for zero mass, and rearward data, (b) zero mass and forward data, (c) same as a, for m=100 eV, (d) same as b, for m=100 eV.

Figure 9: Heuristic examples of two different possibilities for overlap of confidence intervals for forward and rearward fits. a) shows most general possibility, b) shows situation for fits characteristic of this analysis.

Figure 10: Results, for 3 model bursts, of likelihood analysis, for difference in likelihood functions for best fits to forward and rearward signals, as a function of tau neutrino mass. Also displayed is upper limit expected for this difference at the 99% confidence level.

Figure 11: same as figure 8, for two bursts, but reducing the rearward cone to $\cos\theta < 0.80$

Figure 12: Number of late time events for several bursts, showing predicted number based on best fit analysis program plus background, and Poisson probabilities, as a function of neutrino mass.

Figure 13: Poisson probabilities for late time events for two bursts, where the energy cuts E<12, or E<15 MeV have been used, and lower time cutoff has been varied to find the value most sensitive to small tau neutrino mass in this case.

Figure 14: The predicted integrated energy spectrum for events in the forward cone, based on the best fit model to the events generated in a sample burst.

Figure 15: The early time forward cone events for an average luminosity burst.

Table 1: Parameters for 36 models

Model Number	E_{tot} (10^{53} ergs)	t_{mid} (sec)	T_o (MeV)	τ (sec)
1	1.5	0.1	3.0	0.5
2	1.5	0.1	3.0	1.0
3	1.5	0.1	3.0	1.5
4	1.5	0.1	4.0	0.5
5	1.5	0.1	4.0	1.0
6	1.5	0.1	4.0	1.5
7	1.5	1.0	3.0	0.5
8	1.5	1.0	3.0	1.0
9	1.5	1.0	3.0	1.5
10	1.5	1.0	4.0	0.5
11	1.5	1.0	4.0	1.0
12	1.5	1.0	4.0	1.5
13	2.5	0.1	3.0	0.5
14	2.5	0.1	3.0	1.0
15	2.5	0.1	3.0	1.5
16	2.5	0.1	4.0	0.5
17	2.5	0.1	4.0	1.0
18	2.5	0.1	4.0	1.5
19	2.5	1.0	3.0	0.5
20	2.5	1.0	3.0	1.0
21	2.5	1.0	3.0	1.5
22	2.5	1.0	4.0	0.5
23	2.5	1.0	4.0	1.0
24	2.5	1.0	4.0	1.5
25	4.0	0.1	3.0	0.5
26	4.0	0.1	3.0	1.0
27	4.0	0.1	3.0	1.5
28	4.0	0.1	4.0	0.5
29	4.0	0.1	4.0	1.0
30	4.0	0.1	4.0	1.5
31	4.0	1.0	3.0	0.5
32	4.0	1.0	3.0	1.0
33	4.0	1.0	3.0	1.5
34	4.0	1.0	4.0	0.5
35	4.0	1.0	4.0	1.0
36	4.0	1.0	4.0	1.5

Table 1: 36 models of supernova neutrino luminosity and temperature. See text for a description of the temperature and luminosity functions. Note that E_{tot} is the total energy in all species

Table 2: Parameters for ν-e scattering

	A_o	B_o	C_o
$\nu_e+e\rightarrow\nu_e+e$	$(g_V' + g_A')^2$	$(g_V' - g_A')^2$	$g_A'^2 - g_V'^2$
$\bar{\nu}_e+e\rightarrow\bar{\nu}_e+e$	$(g_V' - g_A')^2$	$(g_V' + g_A')^2$	$g_A'^2 - g_V'^2$
$\nu_\mu+e\rightarrow\nu_\mu+e$	$(g_V + g_A)^2$	$(g_V - g_A)^2$	$g_A^2 - g_V^2$
$\bar{\nu}_\mu+e\rightarrow\bar{\nu}_\mu+e$	$(g_V - g_A)^2$	$(g_V + g_A)^2$	$g_A^2 - g_V^2$

Table 2: Parameters for differential and total ν-e scattering cross sections. $g_V = 2\sin^2\theta_W - .5$; $g_A = -.5$; $g_V' = g_V + 1$; $g_A' = g_A + 1$, and θ_W is the weak mixing angle.

Table 3: Expected and Actual Numbers in Forward Cone

Model	Expected Number	$m_\nu = 0$	$m_\nu = 1$ KeV
2	64.947	67	50
	46.843	49	41
5	61.083	53	48
	42.451	39	36
8	59.832	57	51
	41.519	41	38
11	62.066	65	53
	42.121	44	37
14	106.562	112	101
	76.157	78	68
17	98.031	94	76
	68.936	66	52
20	101.070	103	84
	72.511	71	58
23	102.782	108	66
	71.786	78	47
26	170.310	160	130
	121.747	116	90
29	157.888	135	120
	110.975	102	81
32	175.763	184	136
	125.494	128	90
35	161.519	152	119
	112.733	109	73

Table 3: Integrated number in forward cone. For each pair of two lines, top line has energy cut 0<E<15 MeV; bottom line has energy cut 0<E<12 MeV. First column is model number. Second column is expected number, the result of integrating forward cone using parameters fit with backward data. Third column is actual data with $m_\nu = 0$. Fourth column is actual data with $m_\nu = 1$ KeV.

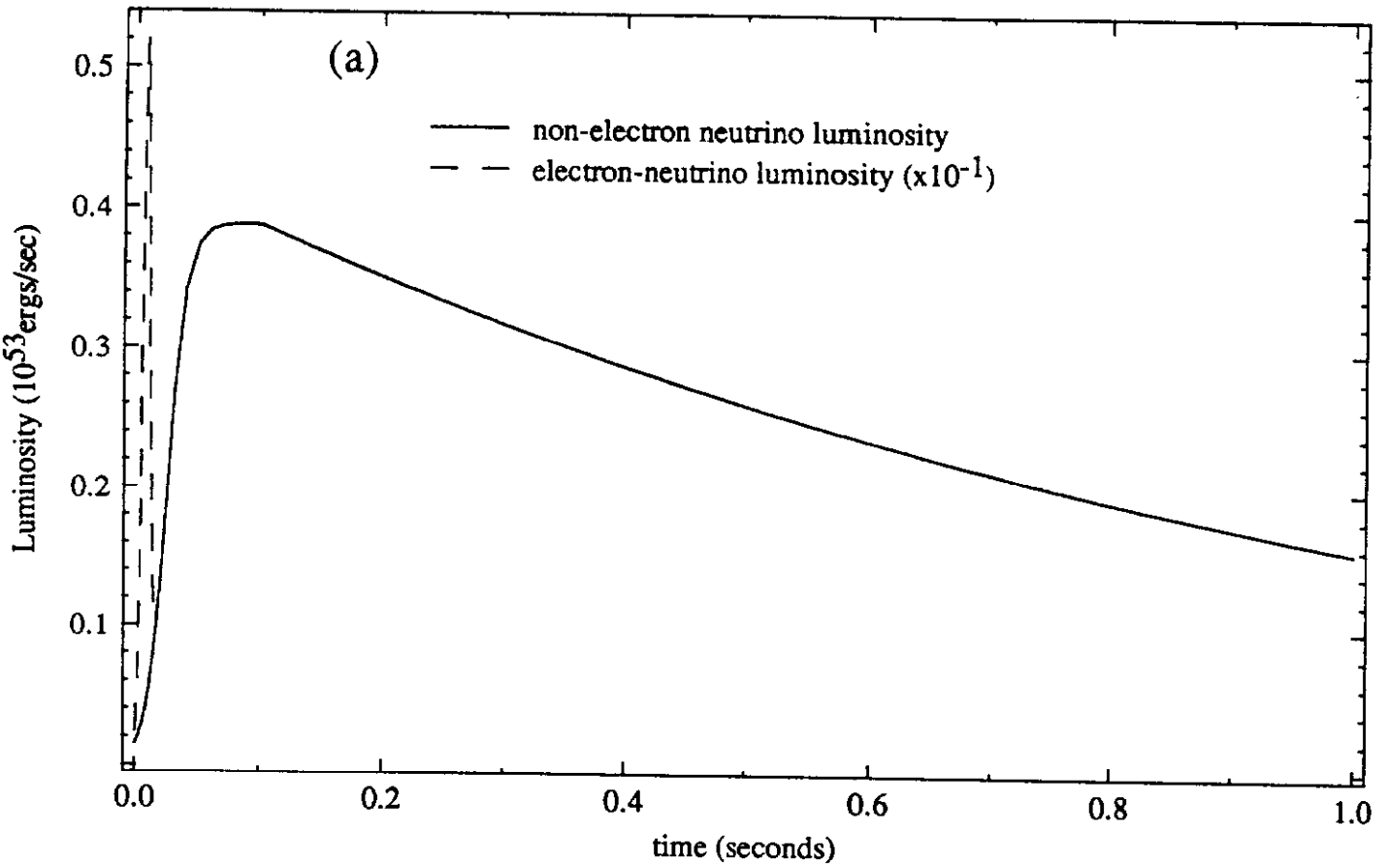
(a)
non-electron neutrino luminosity
electron-neutrino luminosity (x10^{-1})
Luminosity (10^{53}ergs/sec)
0.5
0.4
0.3
0.2
0.1
0.0
0.2
0.4
0.6
0.8
1.0
time (seconds)

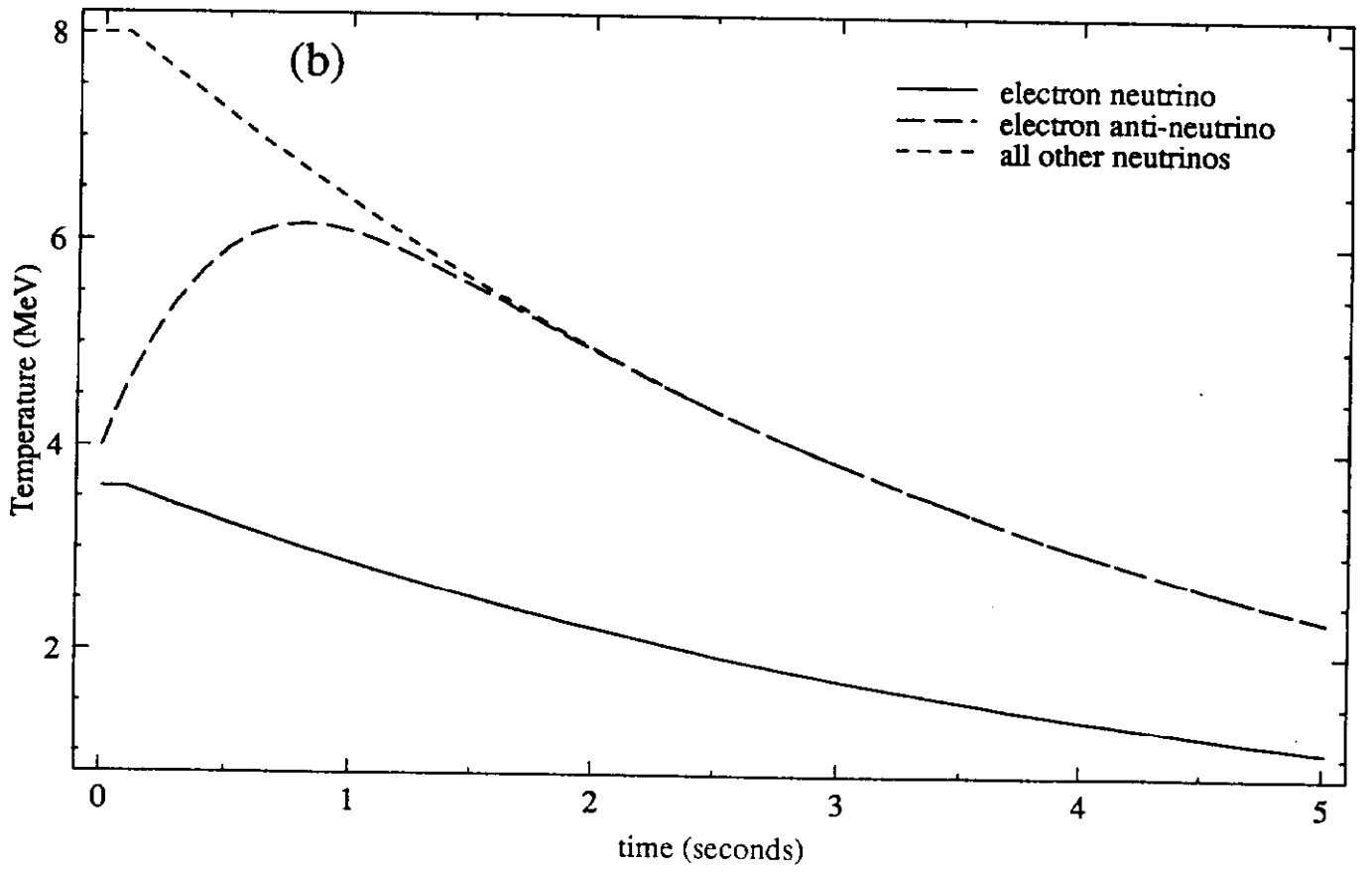
(b)
electron neutrino
electron anti-neutrino
all other neutrinos
Temperature (MeV)
8
6
4
2
0
1
2
3
4
5
time (seconds)

FIGURE 1

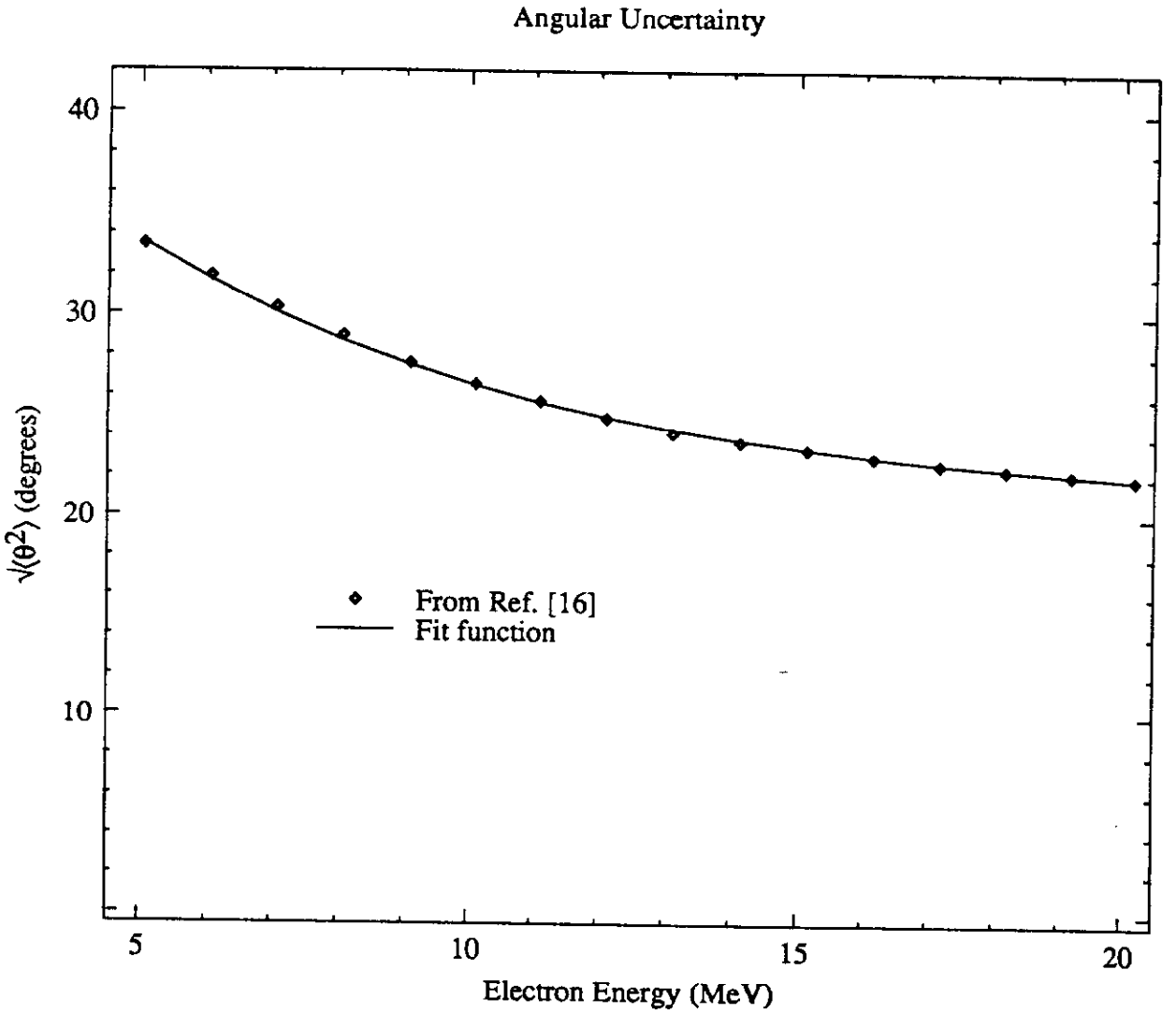
Angular Uncertainty
40
30
20
10
√⟨θ²⟩ (degrees)
From Ref. [16]
Fit function
5
10
15
20
Electron Energy (MeV)

FIGURE 2

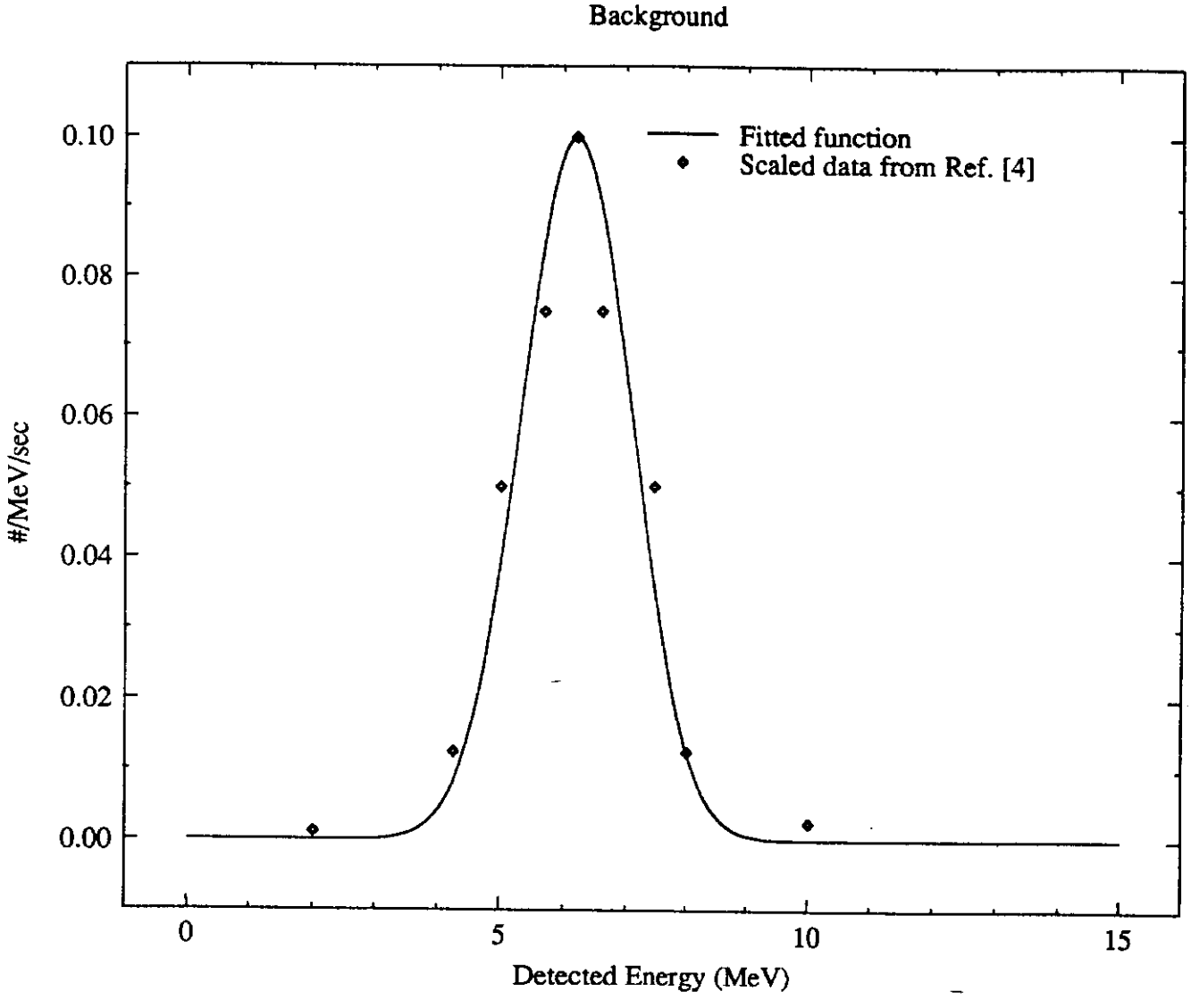
Background
Fitted function
Scaled data from Ref. [4]
0.10
0.08
0.06
0.04
0.02
0.00
#/MeV/sec
0
5
10
15
Detected Energy (MeV)

FIGURE 3

Model 8

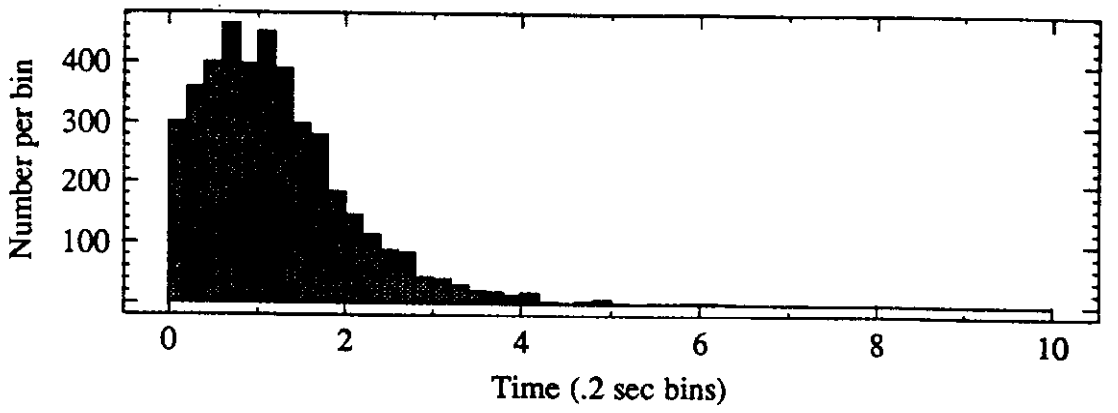

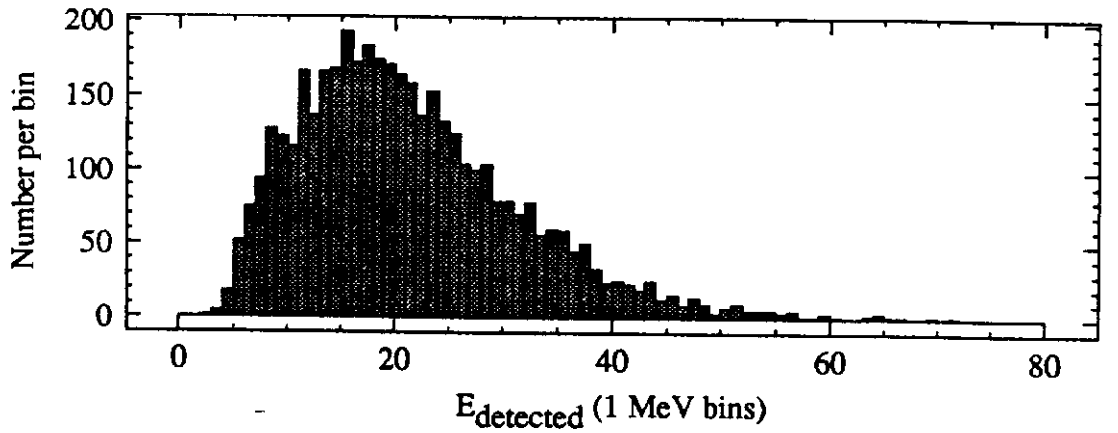

Model 15

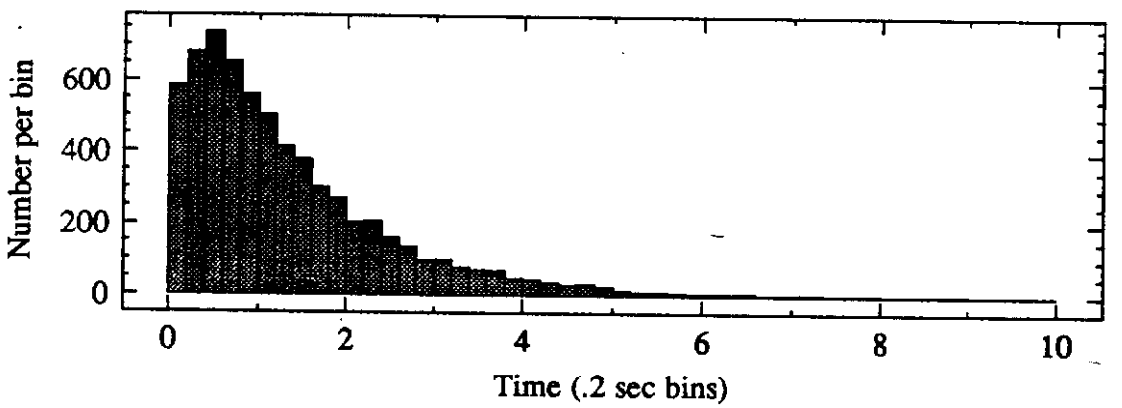

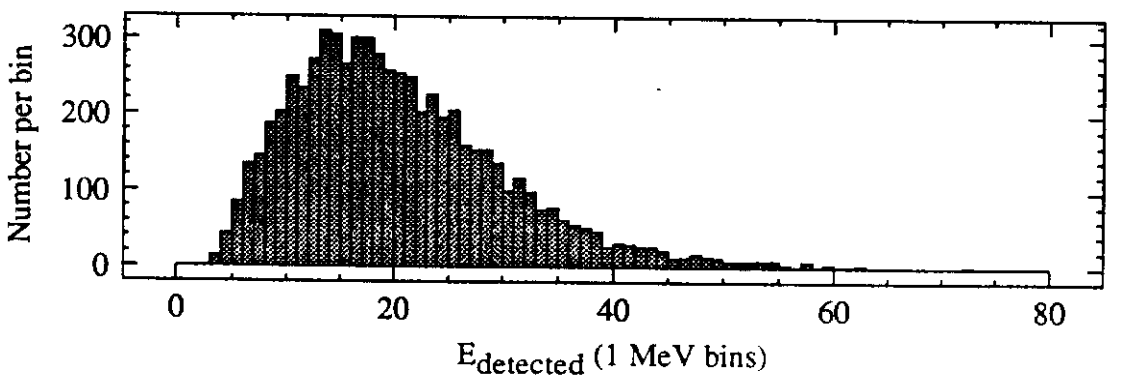

FIGURE 4

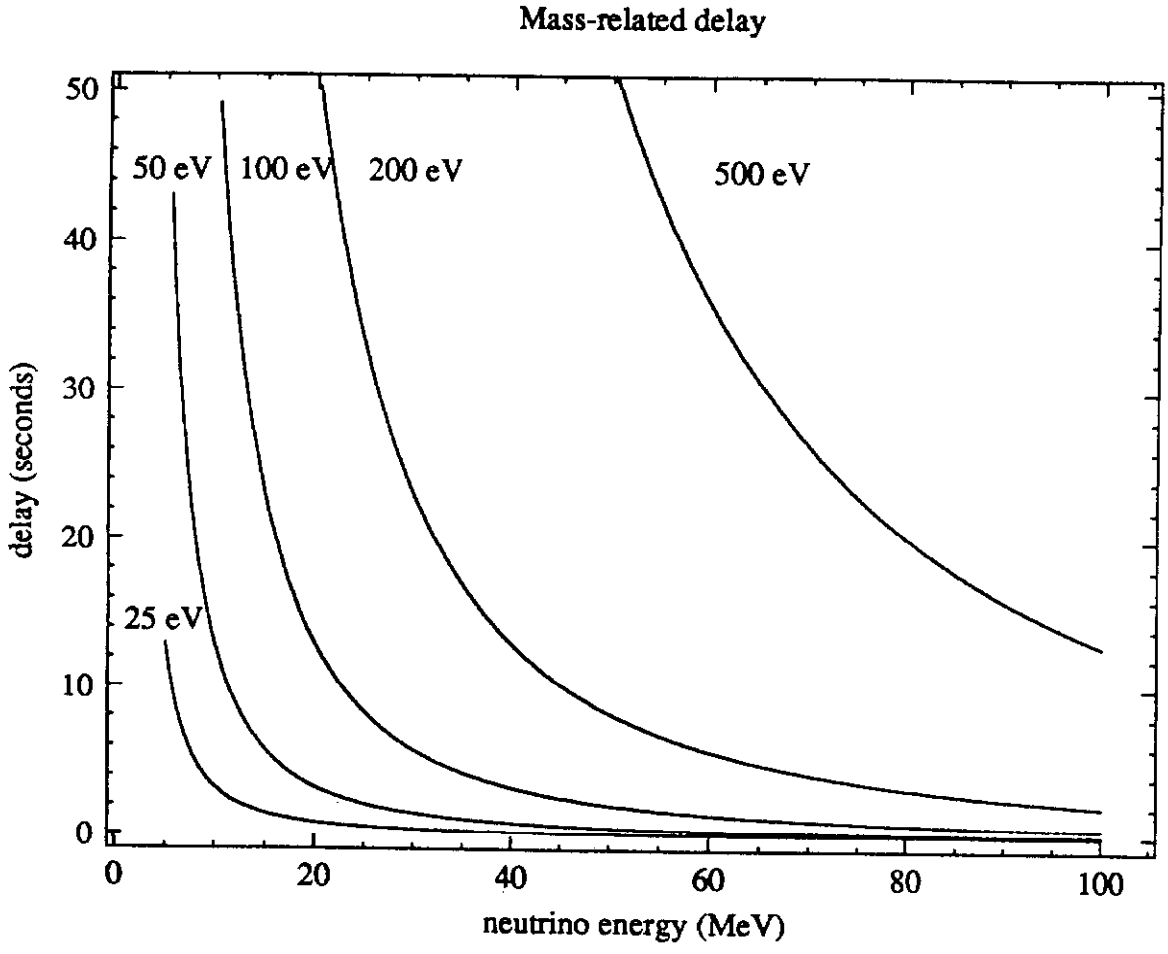
Mass-related delay
50 eV
100 eV
200 eV
500 eV
25 eV
delay (seconds)
neutrino energy (MeV)
0
10
20
30
40
50
0
20
40
60
80
100

FIGURE 5

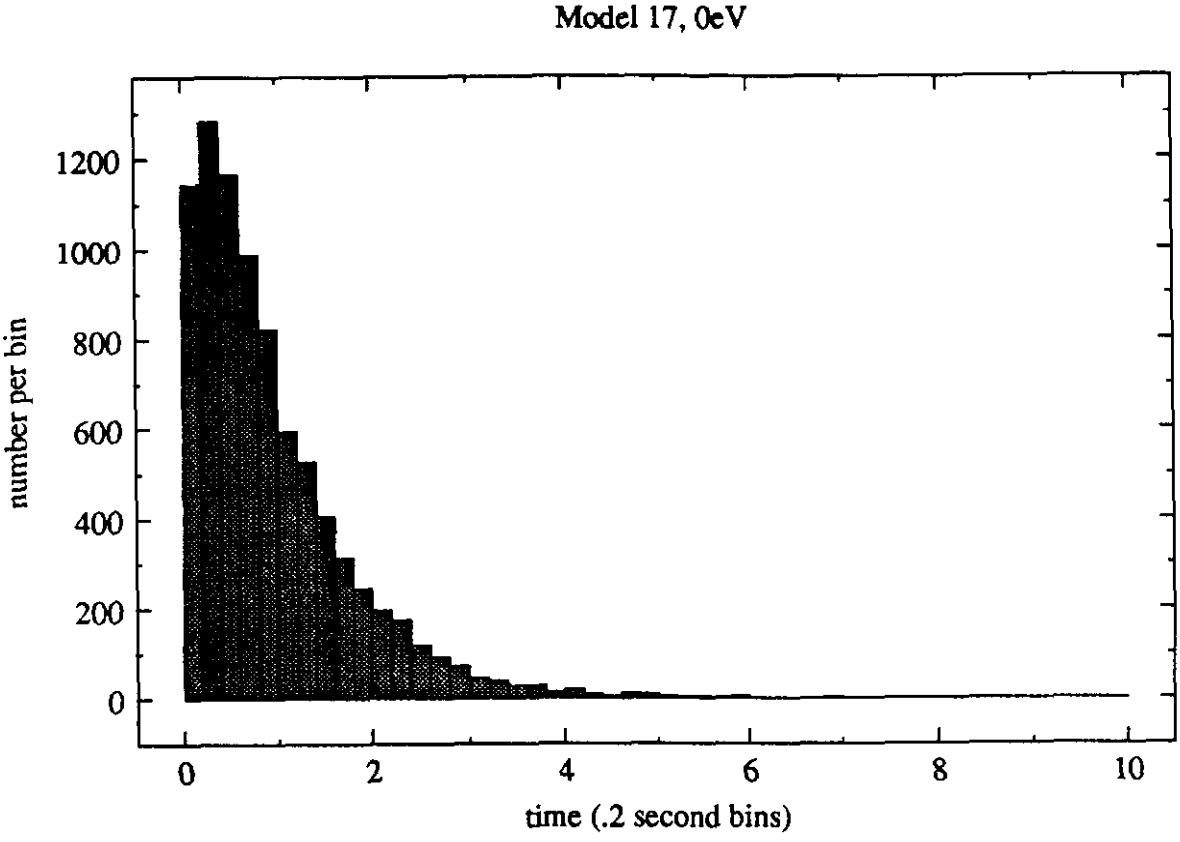
Model 17, 0eV
number per bin
0
200
400
600
800
1000
1200
0
2
4
6
8
10
time (.2 second bins)

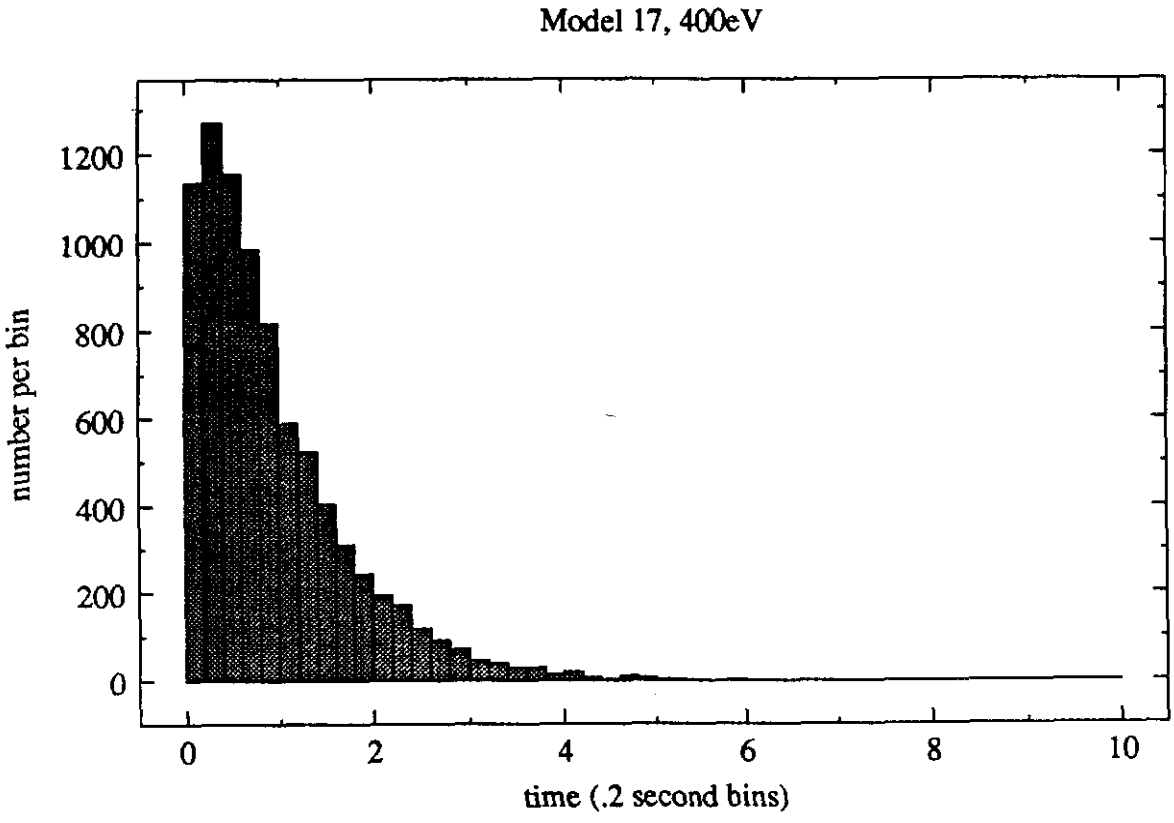
Model 17, 400eV
number per bin
0
200
400
600
800
1000
1200
0
2
4
6
8
10
time (.2 second bins)

FIGURE 6

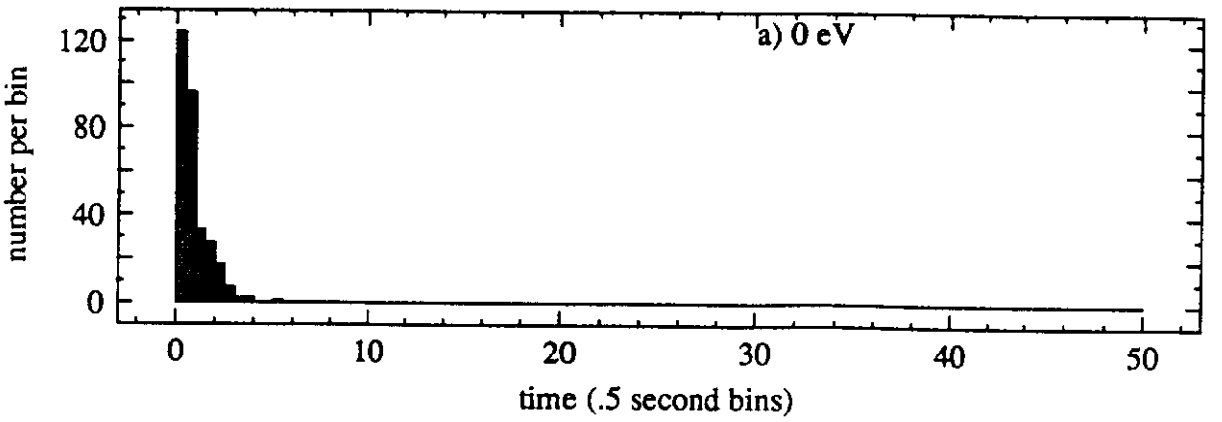
a) 0 eV
number per bin
120
80
40
0
0
10
20
30
40
50
time (.5 second bins)

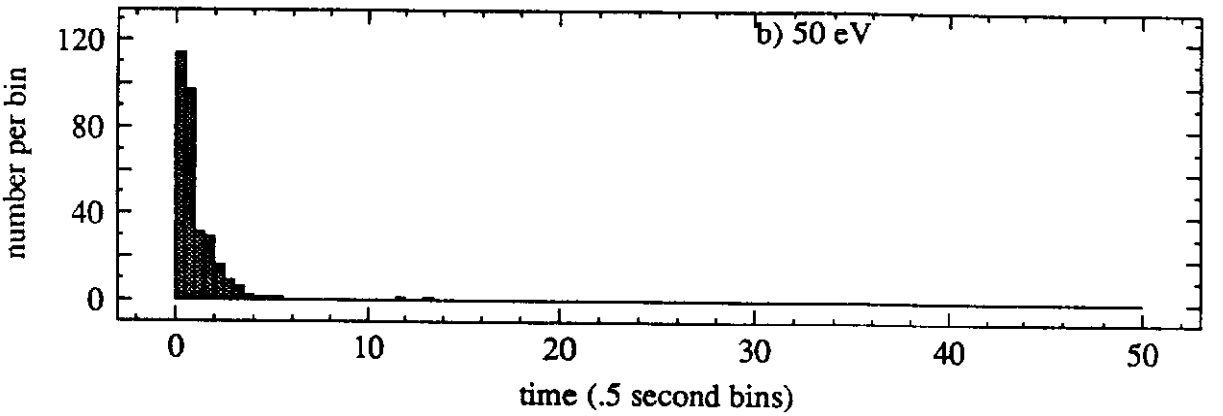
b) 50 eV
number per bin
120
80
40
0
0
10
20
30
40
50
time (.5 second bins)

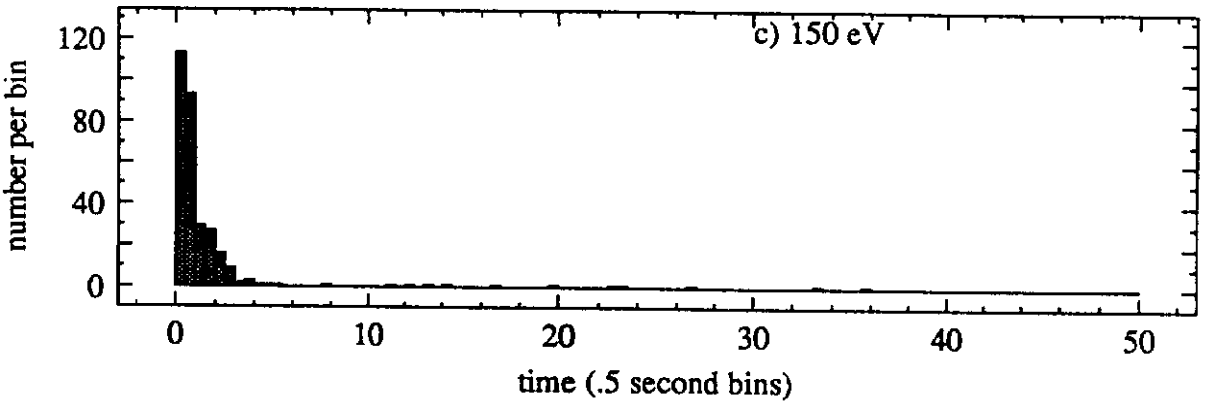
c) 150 eV
number per bin
120
80
40
0
0
10
20
30
40
50
time (.5 second bins)

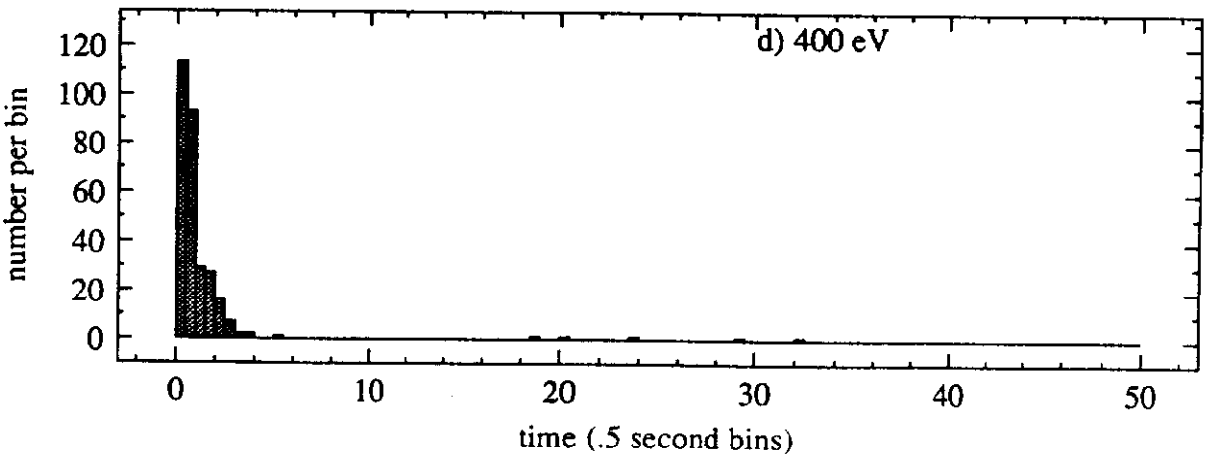
d) 400 eV
number per bin
120
100
80
60
40
20
0
0
10
20
30
40
50
time (.5 second bins)

FIGURE 7

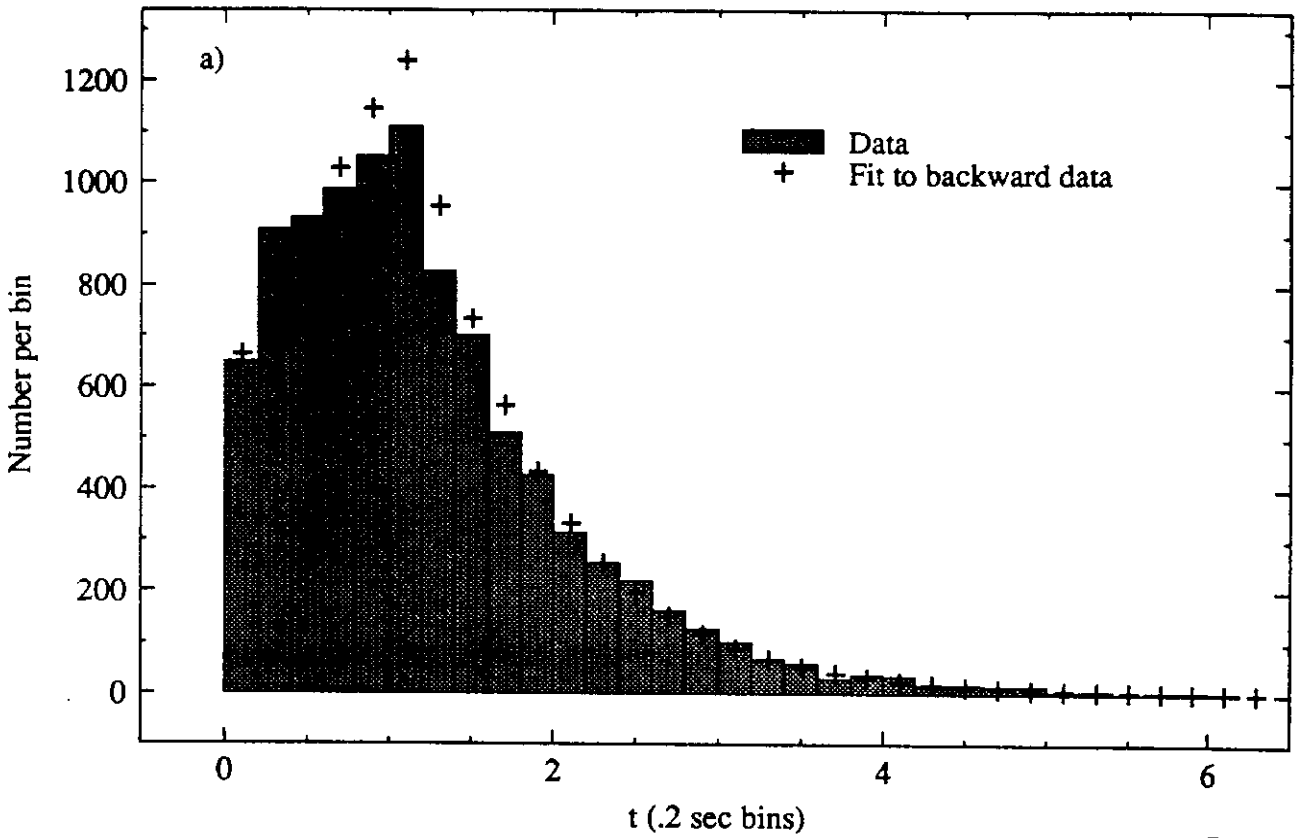

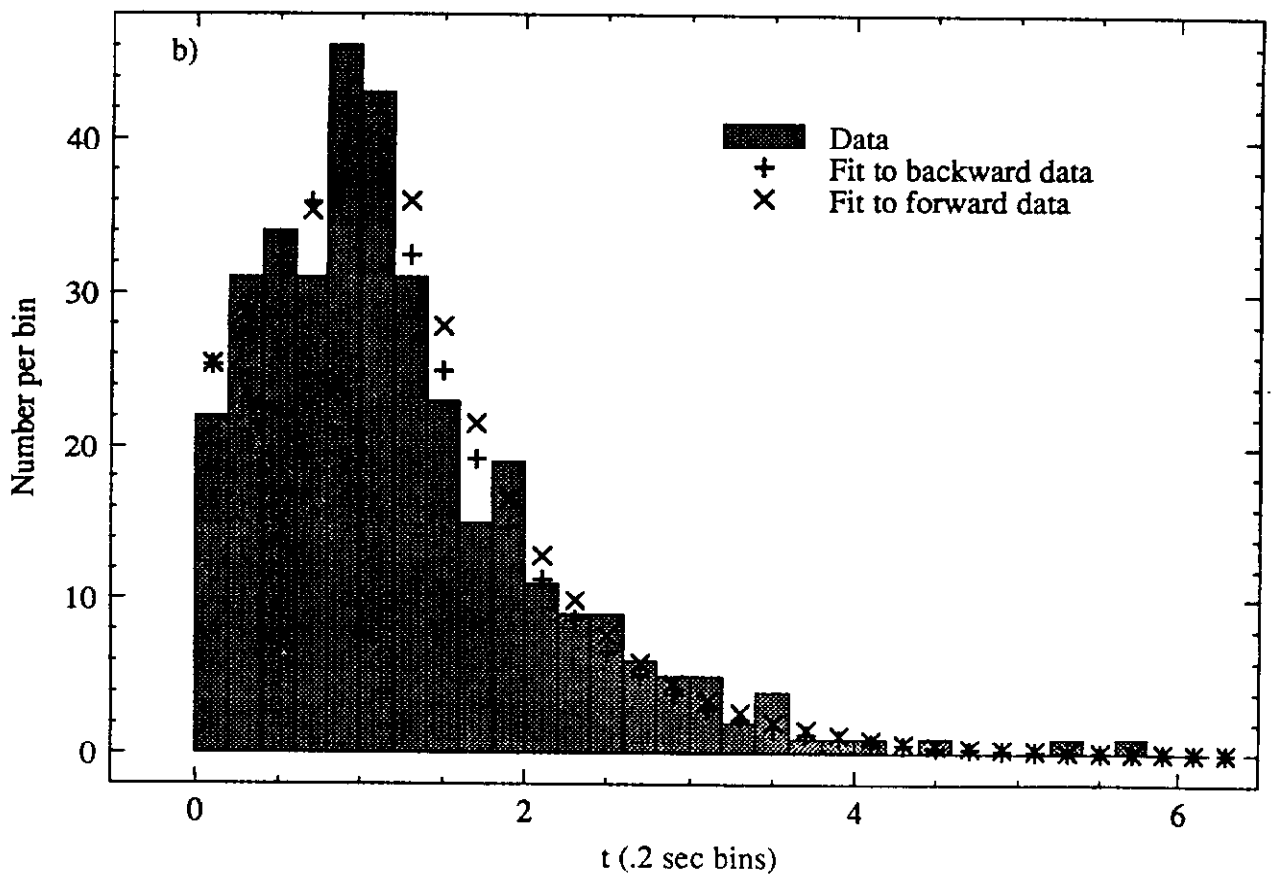

FIGURE 8 (a and b)

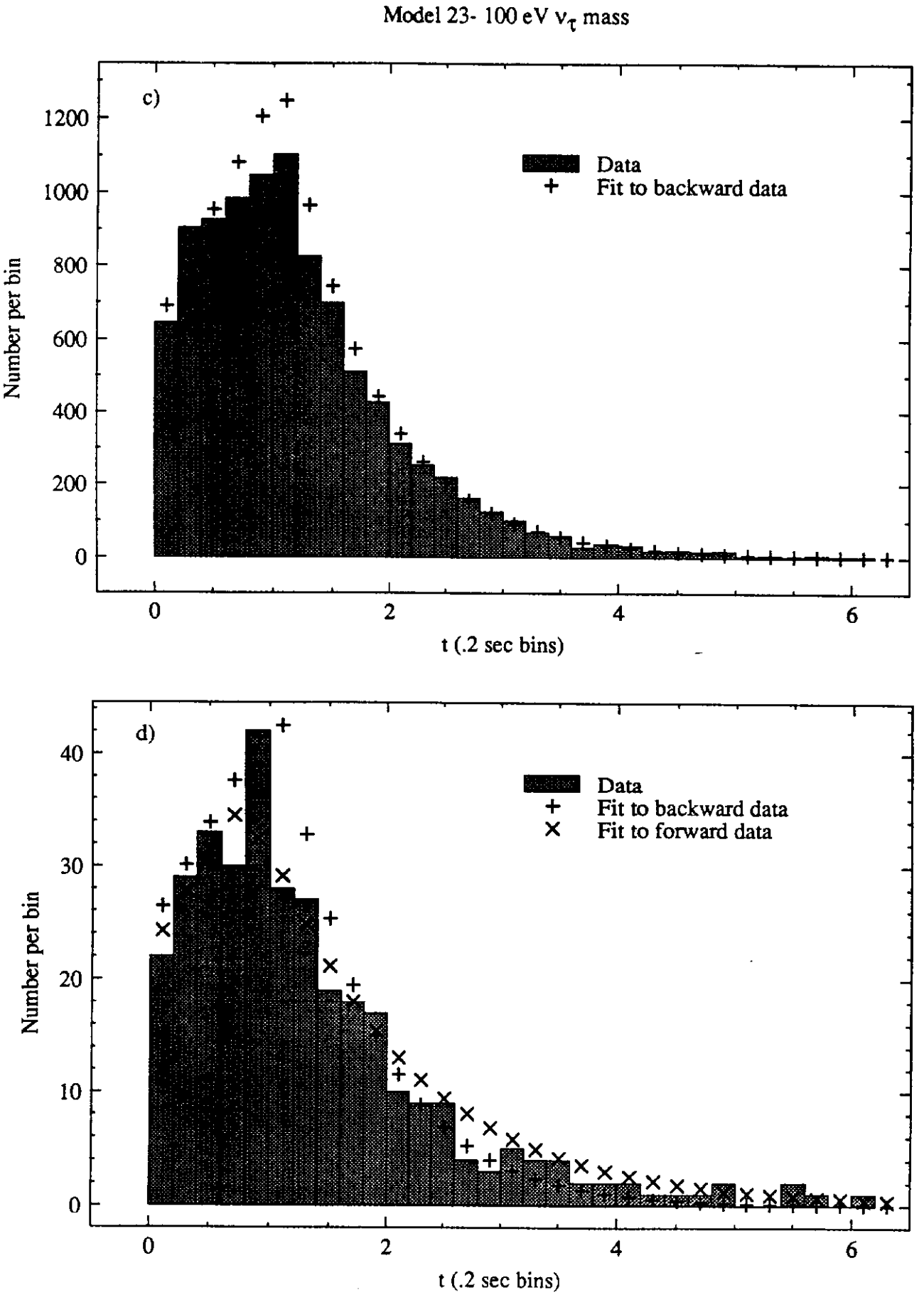

FIGURE 8 (c and d)

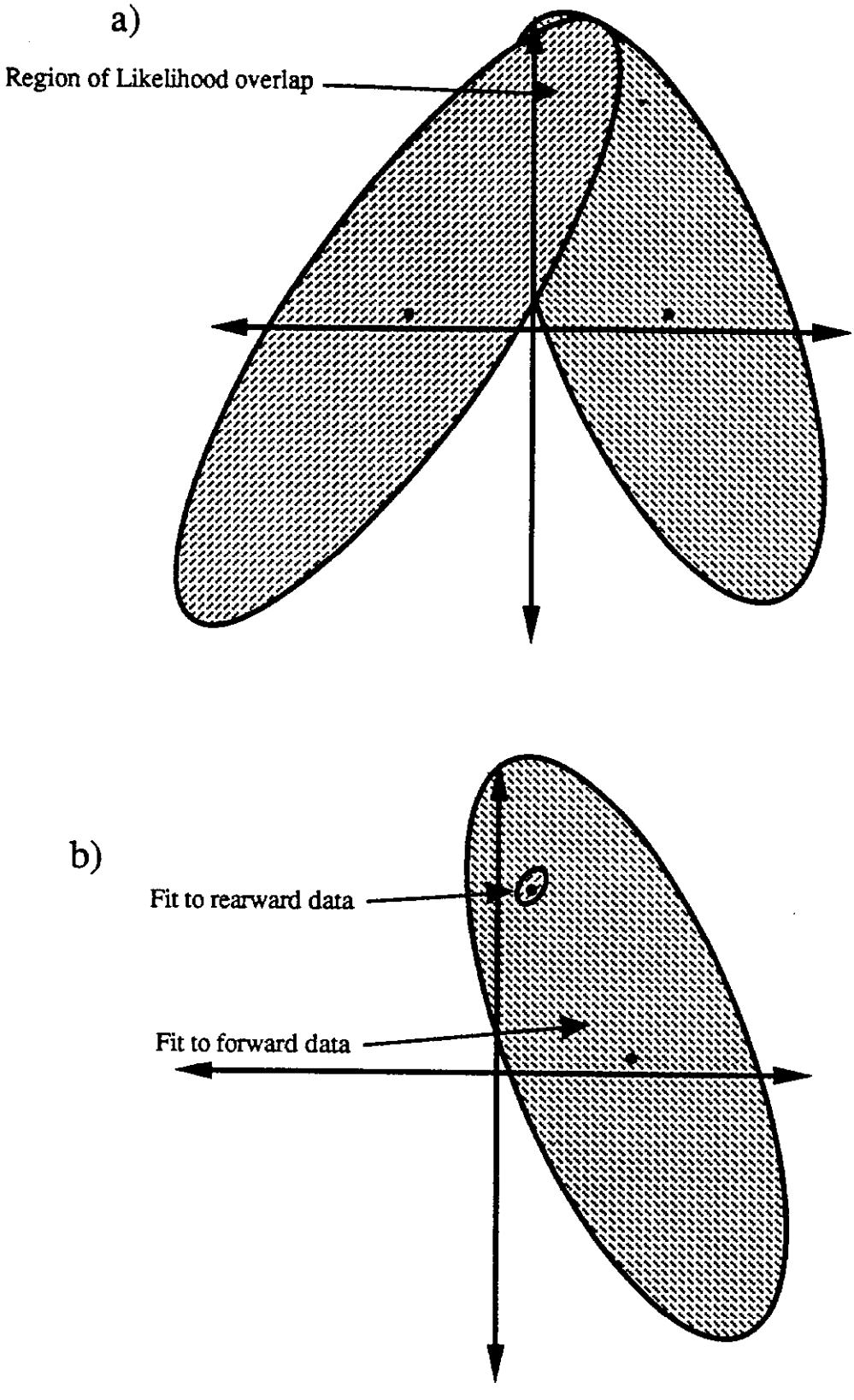
a)
Region of Likelihood overlap
b)
Fit to rearward data
Fit to forward data

FIGURE 9

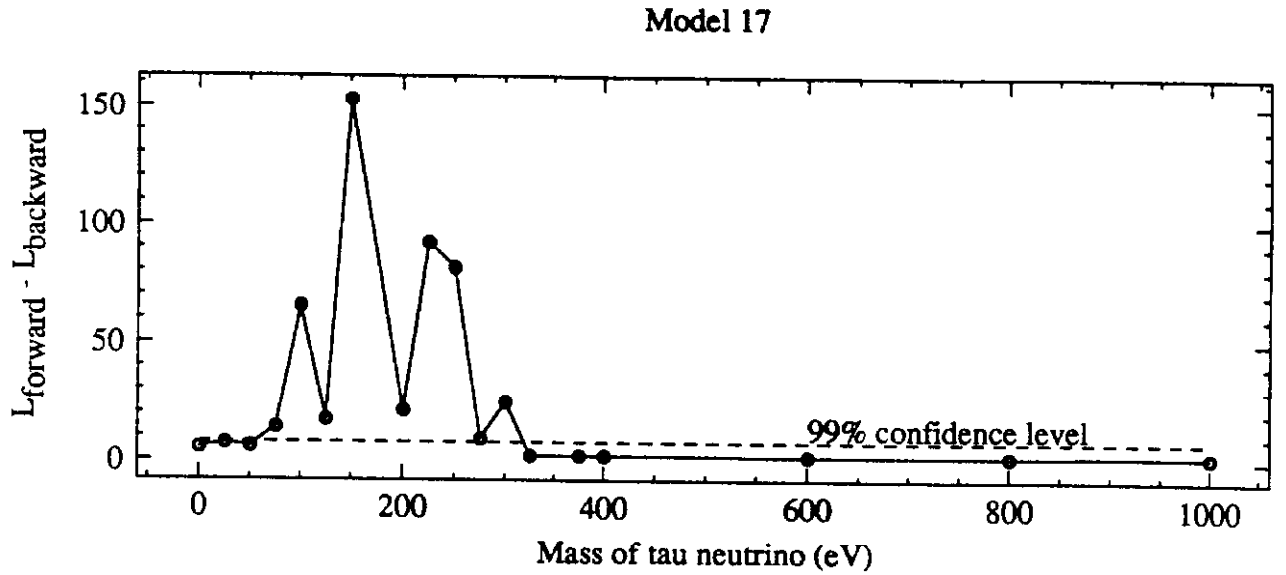
Model 17
150
100
50
0
$L_{forward} - L_{backward}$
99% confidence level
0
200
400
600
800
1000
Mass of tau neutrino (eV)

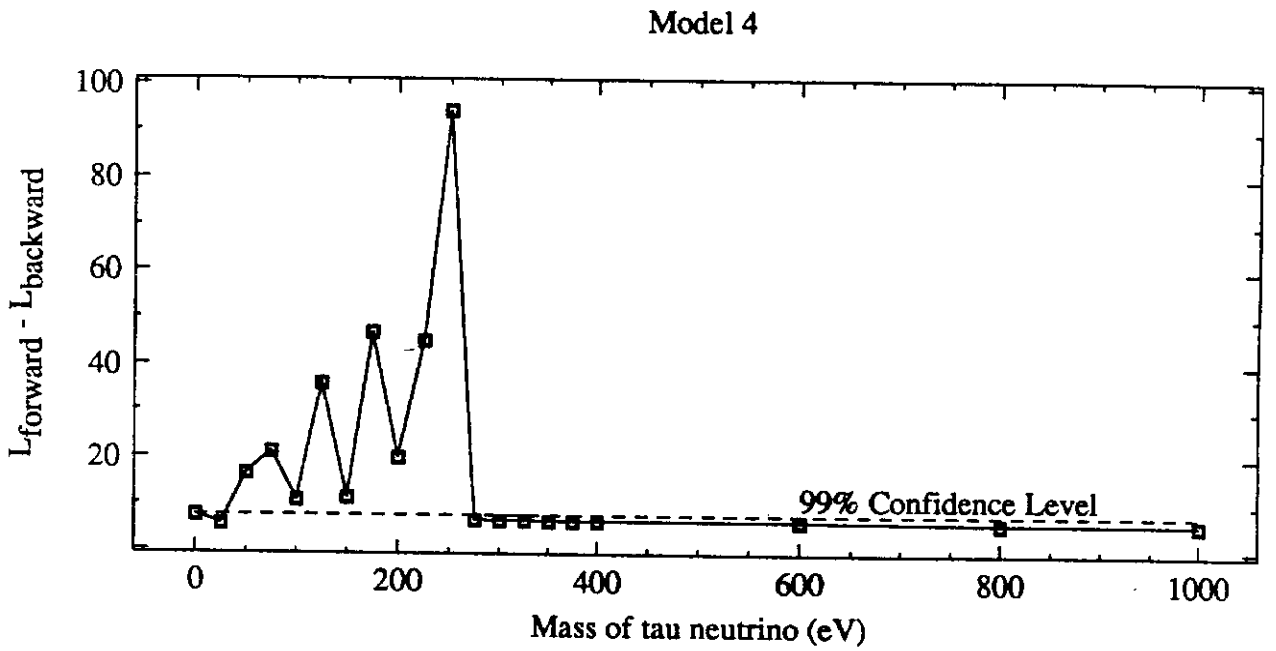
Model 4
100
80
60
40
20
$L_{forward} - L_{backward}$
99% Confidence Level
0
200
400
600
800
1000
Mass of tau neutrino (eV)

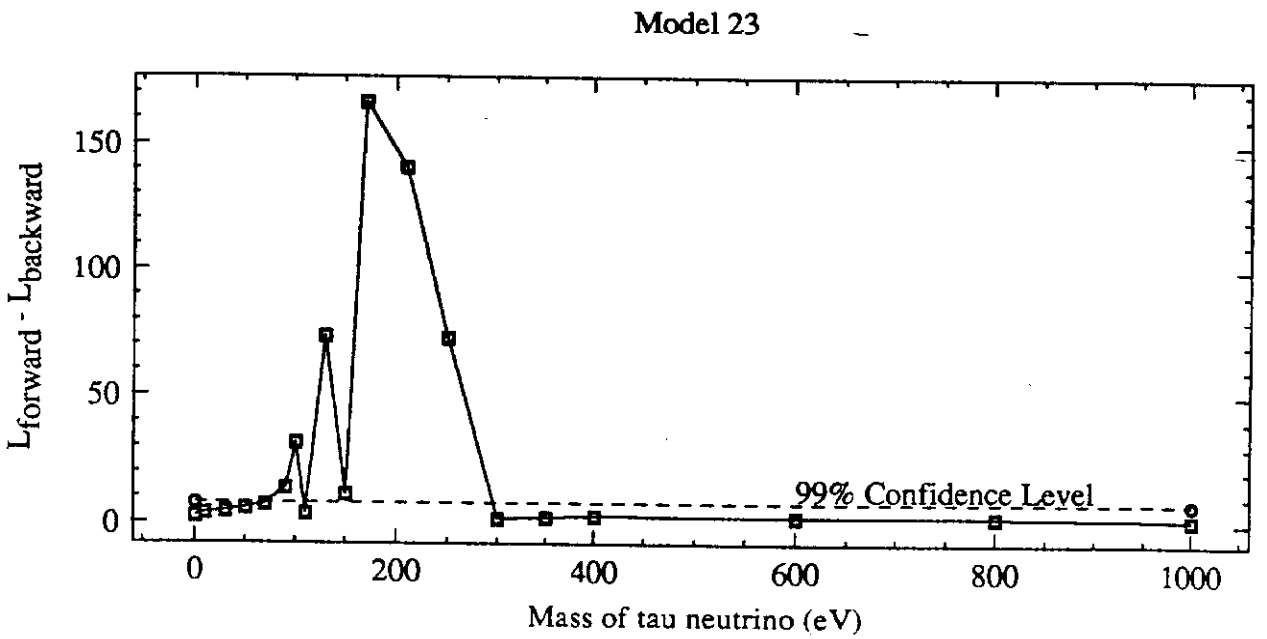
Model 23
150
100
50
0
$L_{forward} - L_{backward}$
99% Confidence Level
0
200
400
600
800
1000
Mass of tau neutrino (eV)

FIGURE 10

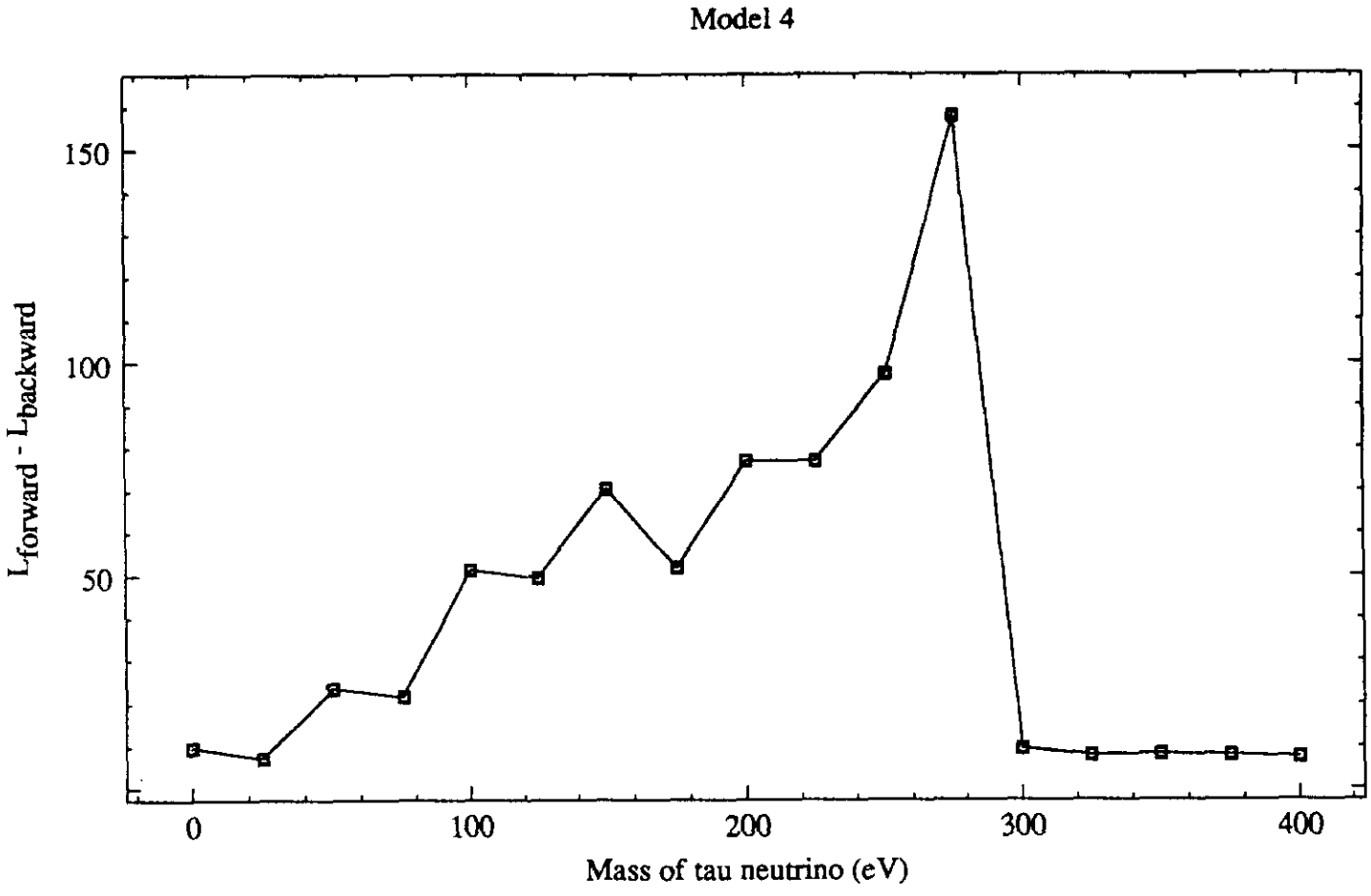
Model 4
150
100
50
$L_{forward} - L_{backward}$
0
100
200
300
400
Mass of tau neutrino (eV)

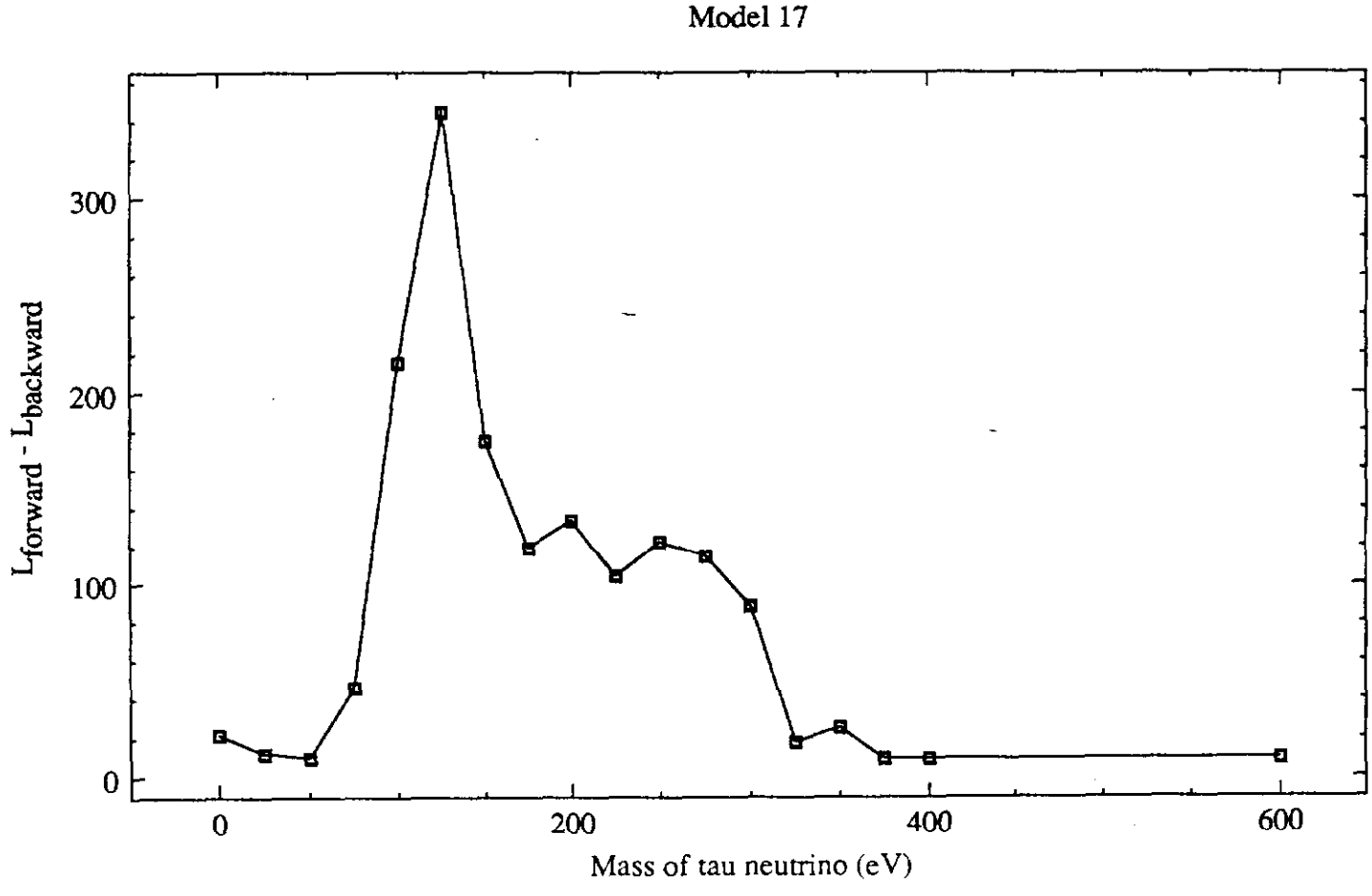
Model 17
300
200
100
0
$L_{forward} - L_{backward}$
0
200
400
600
Mass of tau neutrino (eV)

FIGURE 11

Model 17

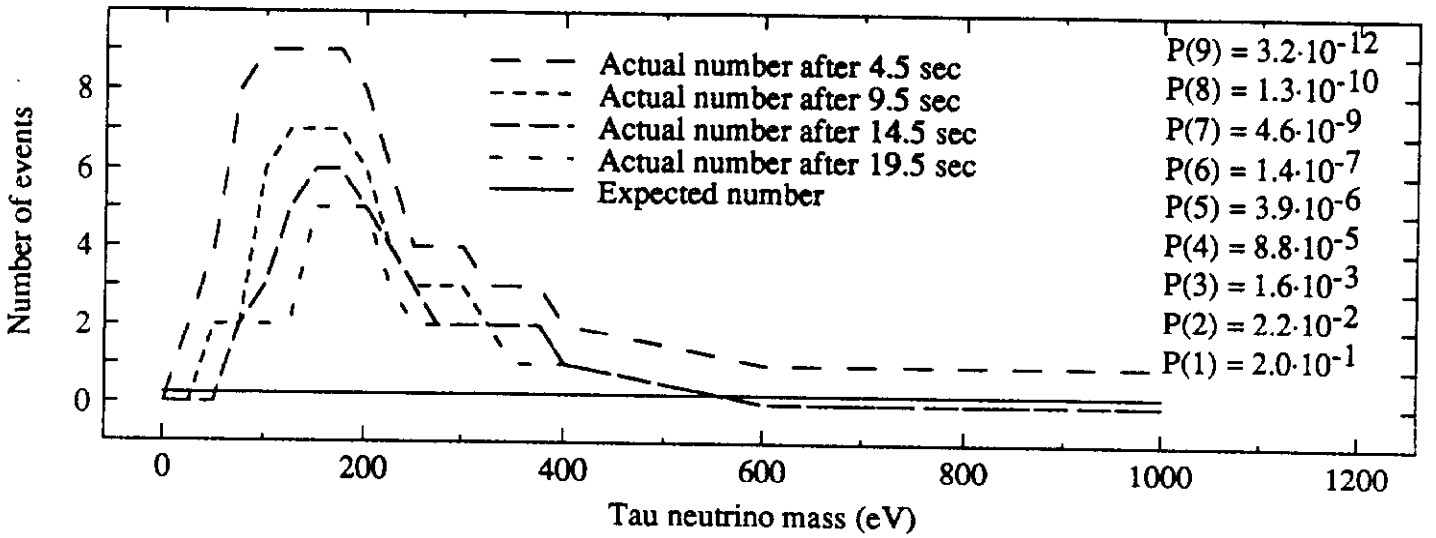

Model 4

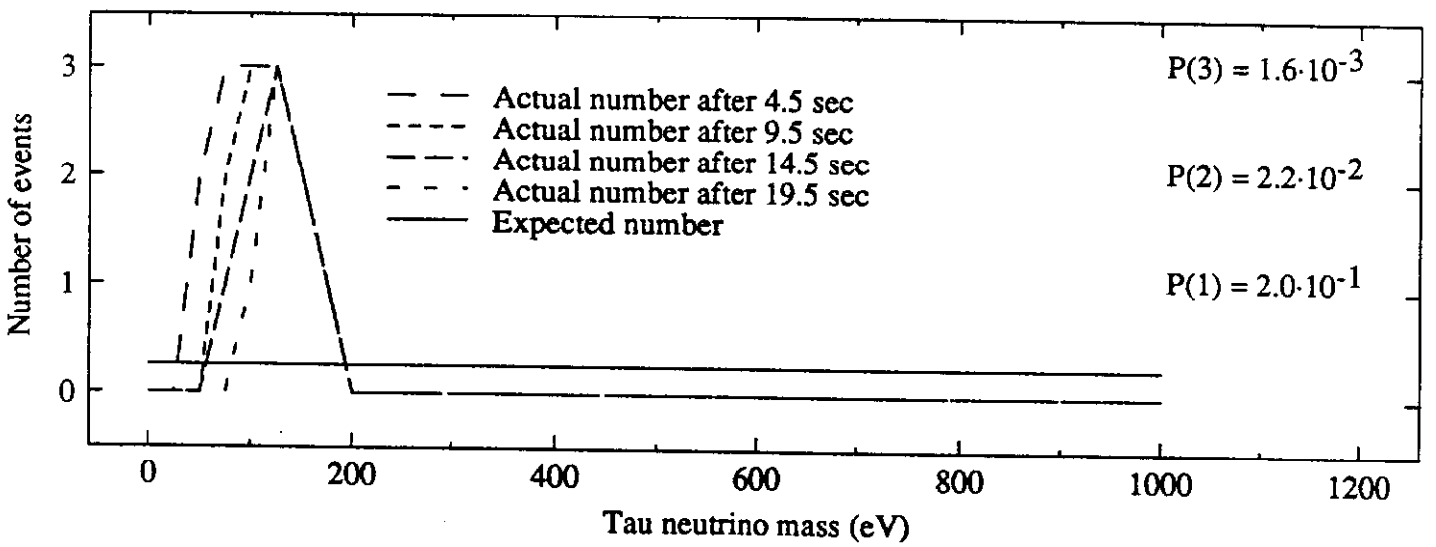

Model 23

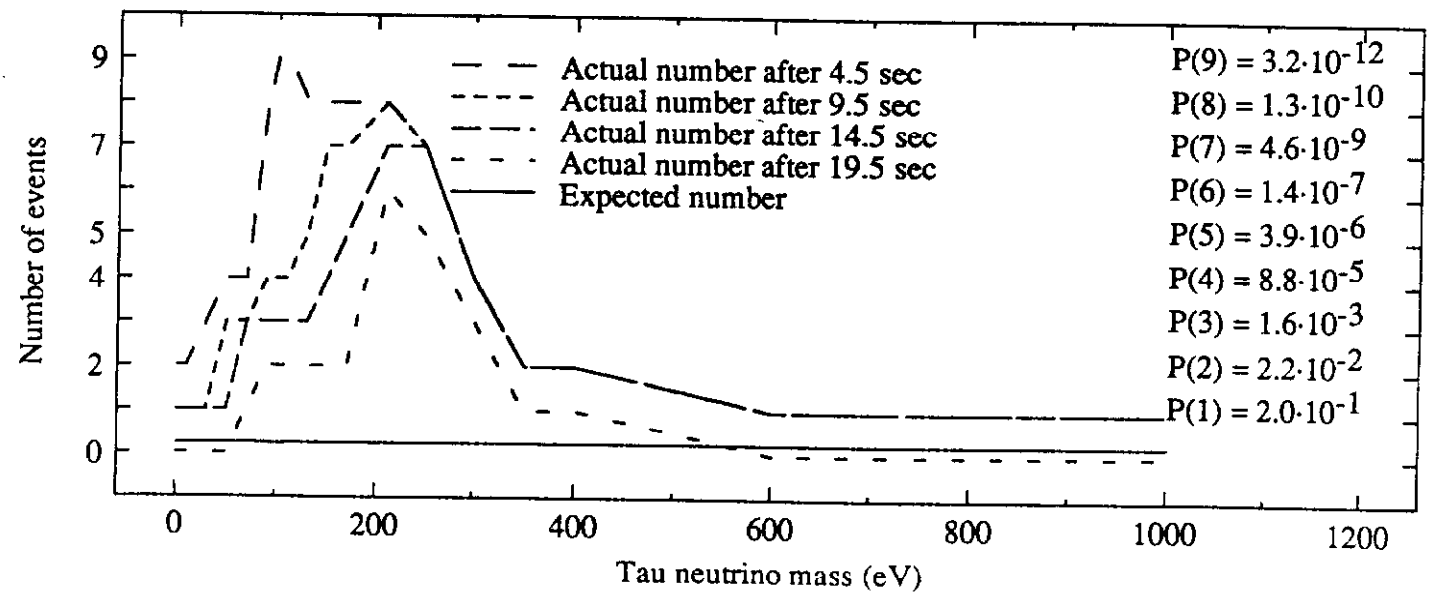

FIGURE 12

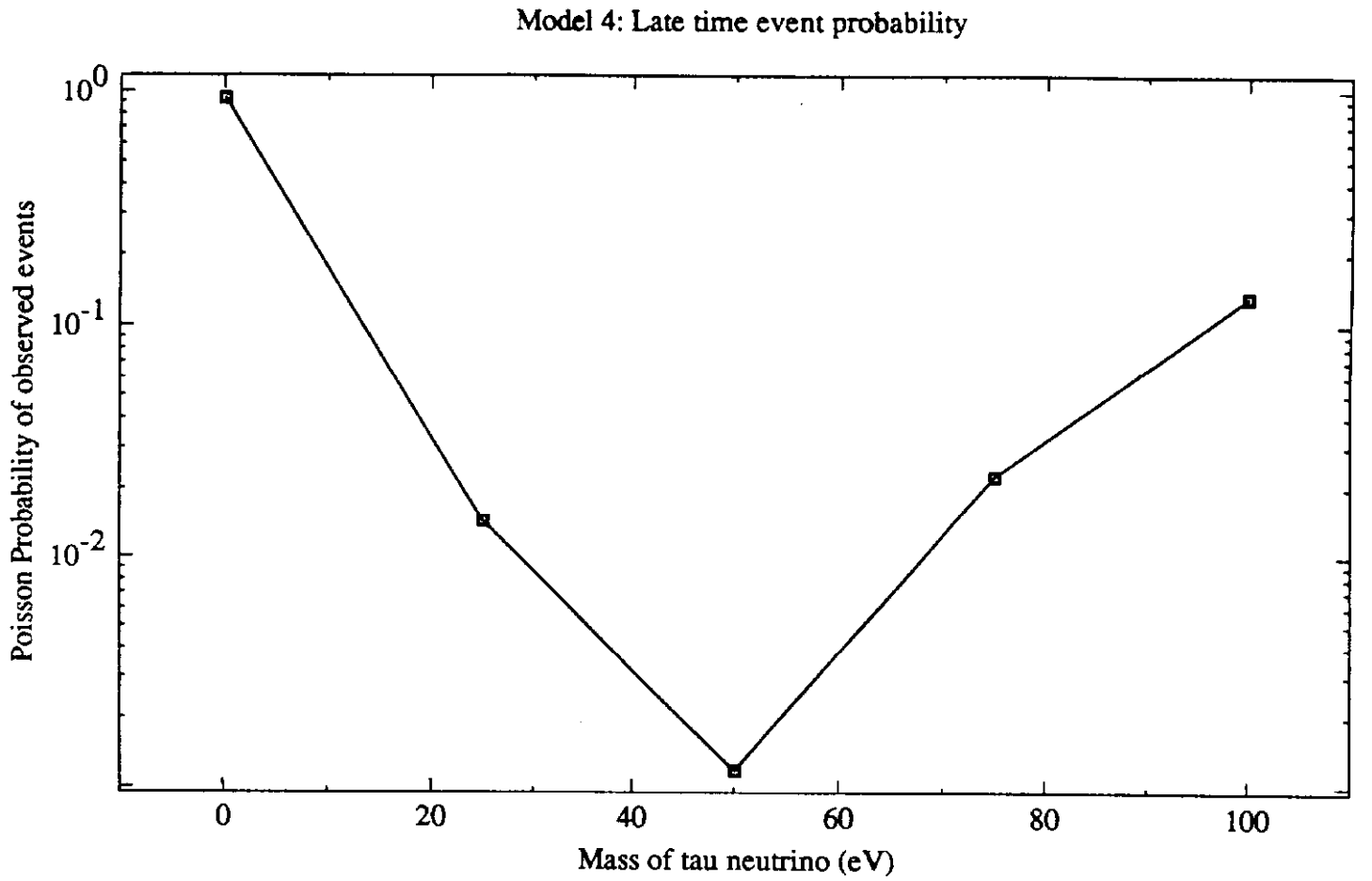
Model 4: Late time event probability
Poisson Probability of observed events
10^0
10^{-1}
10^{-2}
0
20
40
60
80
100
Mass of tau neutrino (eV)

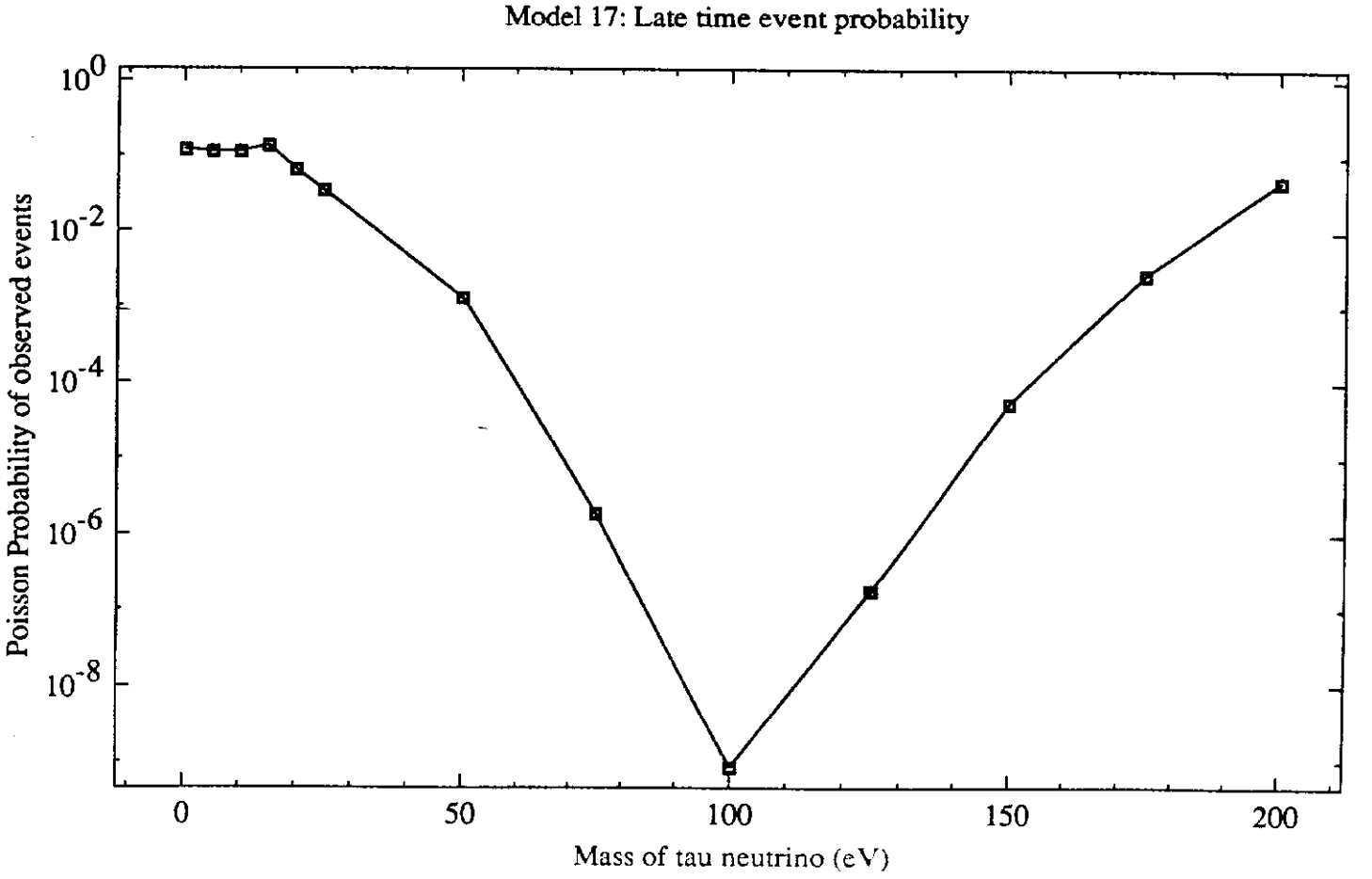
Model 17: Late time event probability
Poisson Probability of observed events
10^0
10^{-2}
10^{-4}
10^{-6}
10^{-8}
0
50
100
150
200
Mass of tau neutrino (eV)

FIGURE 13

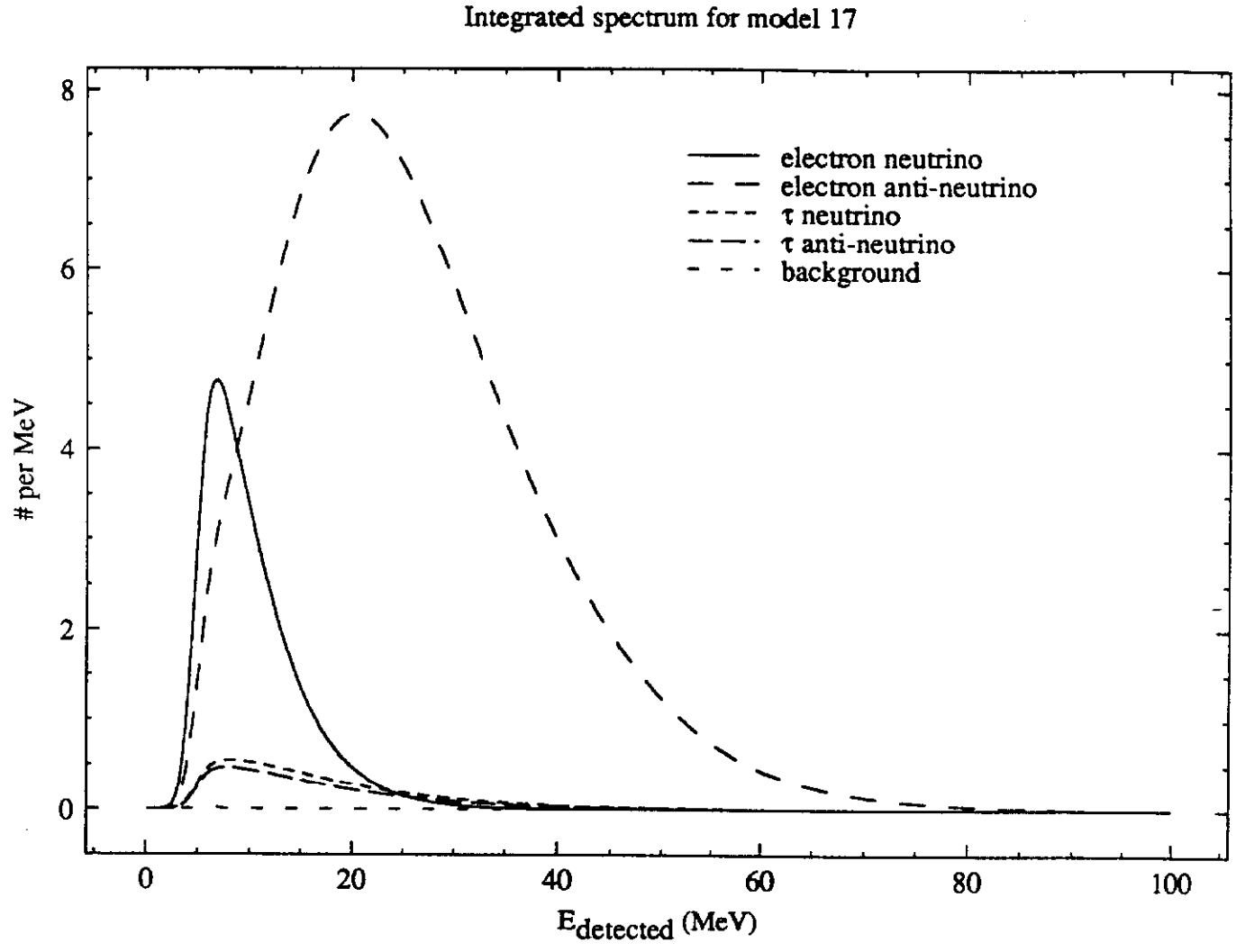
Integrated spectrum for model 17
electron neutrino
electron anti-neutrino
τ neutrino
τ anti-neutrino
background
per MeV
E detected (MeV)
0
2
4
6
8
0
20
40
60
80
100

FIGURE 14

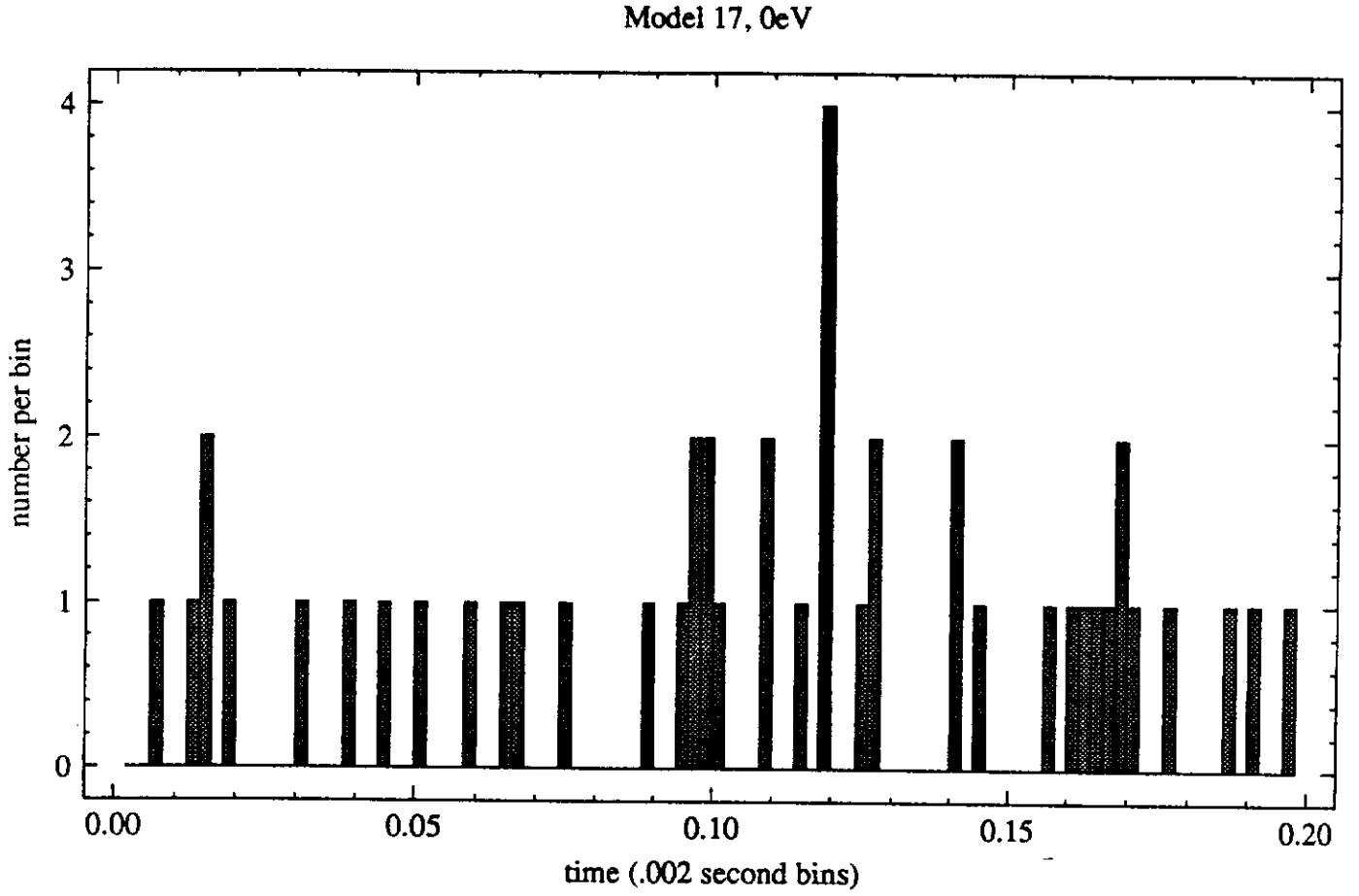
Model 17, 0eV
number per bin
0
1
2
3
4
0.00
0.05
0.10
0.15
0.20
time (.002 second bins)

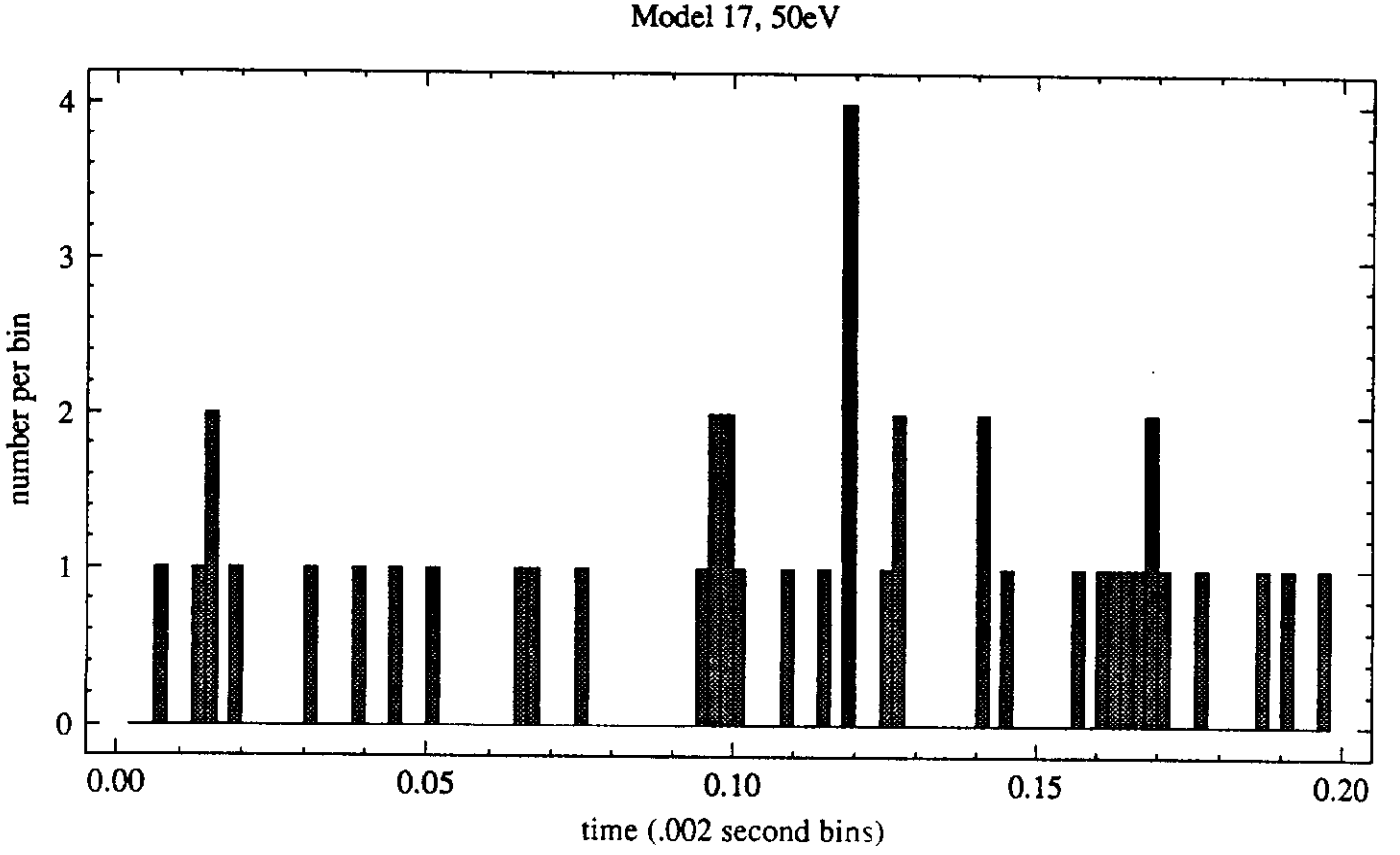
Model 17, 50eV
number per bin
0
1
2
3
4
0.00
0.05
0.10
0.15
0.20
time (.002 second bins)

FIGURE 15